

NASA CR-132481

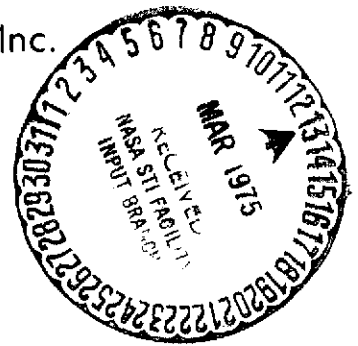


# SINTER OF UNIFORM, PREDICTABLE, BLEMISH-FREE NICKEL PLAQUE FOR LARGE AEROSPACE NICKEL CADMIUM CELLS

(NASA-CR-132481) SINTER OF UNIFORM, PREDICTABLE, BLEMISH-FREE NICKEL PLAQUE FOR LARGE AEROSPACE NICKEL CADMIUM CELLS (Heliotek) 75 p HC \$4.25 CACL 10A N75-18717 Unclas 63/44 11725

by Harvey N. Seiger

HELIOTEK Divison of TEXTRON Inc.  
12500 Gladstone Avenue  
Sylmar, California 91342



prepared for  
NATIONAL AERONAUTICS AND SPACE ADMINISTRATION  
under Contract NAS1-10694

NASA Langley Research Center  
Hampton, Virginia

1. Report No. NASA CR-132481		2. Government Accession No.		3. Recipient's Catalog No.	
4. Title and Subtitle SINTER OF UNIFORM, PREDICTABLE, BLEMISH-FREE NICKEL PLAQUE FOR LARGE AEROSPACE NICKEL CADMIUM CELLS				5. Report Date February, 1975	
				6. Performing Organization Code	
7. Author(s) Harvey N. Seiger				8. Performing Organization Report No.	
9. Performing Organization Name and Address Heliotek Division of Textron 12500 Gladstone Ave. Sylmar, California 91342				10. Work Unit No.	
				11. Contract or Grant No. NAS 1-10694	
12. Sponsoring Agency Name and Address National Aeronautics and Space Administration NASA-Langley Research Center Hampton, Virginia 23365				13. Type of Report and Period Covered Contractor Report	
				14. Sponsoring Agency Code	
15. Supplementary Notes					
16. Abstract An empirical program was carried out to fabricate sintered nickel plaque that is uniform, reproducible and blemish-free. A series of nickel slurry compositions were tested. Important slurry parameters were found to be the nature of the binder, a pore former and the method of mixing. A slow roll mixing which is non-turbulent successfully eliminated entrapped air so that bubbles and pockets were avoided in the sinter. A slurry applicator was developed which enabled an equal quantity of slurry to be applied to both sides of the grid. The volume of slurry applied is dependent upon the spacing of the doctor blades, the inclination angle, viscosity and composition of the slurry and the pulling rate. Slow drying of the slurry eliminates mud cracking. Cleaning of the grid eliminated air entrapment at the perforations and improved sinter adhesion. Sintering in a furnace having a graded atmosphere characteristic, ranging from oxidizing to strongly reducing, improved adhesion of porous sinter to grid and resulted in a uniform welding of nickel particles to each other throughout the plaque. Sintering was carried out in a horizontal furnace having three heating zones and 16 heating control circuits. The temperature profile in the first zone is ramp-shaped while in the other two zones the temperature profile is essentially flat. Eight tests were used for plaque evaluation. These included (1) appearance, (2) grid location and adhesion, (3) mechanical strength, (4) thickness, (5) weight per unit area, (6) void volume per unit area, (7) surface area and (8) electrical resistance. The processes developed were used to manufacture plaques, samples of which were delivered to NASA Langley Research Center. Plaque material was impregnated using Heliotek proprietary processes and 100 AH cells were fabricated. Plates and sealed cells were delivered to NASA Langley Research Center.					
17. Key Words (Suggested by Author(s)) Nickel Cadmium Cell Sintered nickel plaque Wet slurry process One hundred AH cell			18. Distribution Statement  Unclassified - unlimited		
19. Security Classif. (of this report) Unclassified		20. Security Classif. (of this page) Unclassified		21. No. of Pages 75	22. Price*

\* For sale by the National Technical Information Service, Springfield, Virginia 22151

Sinter of Uniform, Predictable, Blemish-Free  
Nickel Plaque for Large Aerospace Nickel Cadmium Cells

by

Harvey N. Seiger, Heliotek/Textron

Prepared under Contract NAS1-10694

Heliotek, Division of Textron Inc.

12500 Gladstone Avenue

Sylmar, California 91342

for

National Aeronautics and Space Administration

TABLE OF CONTENTS

		<u>PAGE NO.</u>
I	SUMMARY	1
II	INTRODUCTION	3
III	EXPERIMENTAL	5
IV	TEST PROCEDURES	25
V	TEST RESULTS	41
VI	100 AH CELL DESIGN	51
VII	NEW TECHNOLOGY	64
VIII	CONCLUDING REMARKS	67
IX	RECOMMENDATIONS	69
X	ACKNOWLEDGEMENTS	70
XI	APPENDIX	71

LIST OF FIGURES

FIGURE		PAGE NO.
1	Grid Cleaning Apparatus	7
2	Stainless Steel Drum and Roller Bearing Mill for Slurry Deaeration and Homogenizing	14
3	Moyno Pump Modified for Slurry Transfer	16
4	Grid coating Apparatus	17
5	Horizontal Sintering Furnace	20
6	Temperature Profile in Sintering Furnace	22
7	Plaque Cutting Shears	24
8	Plaque Hardness Testing Apparatus	29
9	Test Cell for Double Layer Capacitance Measurements	32
10	Experimental Set-up For Voltage Step Measurements	33
11	Current-Time Behavior as a Function of Biased Pulse Base Potential	35
12	Current-Time Response as a Function of Voltage Pulse Amplitude	36
13	Peak Current as Function of Voltage Pulse Amplitude	37
14	Multipoint Resistance Probe	39
15	Discharge Curve	57
16	Discharge Curve	58
17	Effect of Charge Rate on Capacity	60
18	End of Charge Pressure	61
19	Pressure Decay	62
A-1-a	Capacity Dependence on Sinter Porosity	73

LIST OF TABLES

TABLE		PAGE NO.
1	Basic Material for Porous Nickel Plaque	4
1A	Slurry Compositions for Plaque	11
2	Target Parameter for Sintered Plaque	42
3	Factorial Experiment for Sintering Positive Plaque	43
4	Summary of Plaque Measurements	44
5	Summary of Data Analysis	46
6A	Plaque Processed for 100 AH Cells	48
6B	Negative Electrode Impregnation Data	49
6C	Positive Electrode Impregnation Data	50
7	HNC 100.3 Cell Design	54

Sinter of Uniform, Predictable, Blemish-Free  
Nickel Plaque for Large Aerospace Nickel Cadmium Cells

by

Harvey N. Seiger, Heliotek/Textron

S U M M A R Y

An empirical program was carried out to fabricate sintered nickel plaque that is uniform, reproducible and blemish-free. A series of nickel slurry compositions were tested. Important slurry parameters were found to be the nature of the binder, a pore former and the method of mixing. A slow roll mixing which is non-turbulent successfully eliminated entrapped air so that bubbles and pockets were avoided in the sinter.

A slurry applicator was developed which enabled an equal quantity of slurry to be applied to both sides of the grid. The volume of slurry applied is dependent upon the spacing of the doctor blades, the inclination angle, viscosity and composition of the slurry and the pulling rate.

Slow drying of the slurry eliminates mud cracking. Cleaning of the grid eliminated air entrapment at the perforations and improved sinter adhesion. Sintering in a furnace having a graded atmosphere characteristic, ranging from oxidizing to strongly reducing, improved adhesion of porous sinter to grid and resulted in a uniform welding of nickel particles to each other throughout the plaque.

Sintering was carried out in a horizontal furnace having three heating zones and 16 heating control circuits. The temperature profile in the first zone is ramp-shaped while in the other two zones the temperature profile is essentially flat.

Eight tests were used for plaque evaluation. These included (1) appearance, (2) grid location and adhesion, (3) mechanical strength, (4) thickness, (5) weight per unit area, (6) void volume per unit area, (7) surface area and (8) electrical resistance.

The processes developed were used to manufacture plaques, samples of which were delivered to NASA Langley Research Center. Plaque material was impregnated using Heliotek proprietary processes and 100 AH cells were fabricated. Plates and sealed cells were delivered to NASA Langley Research Center.



## I N T R O D U C T I O N

The obtaining of highly reliable secondary nickel cadmium battery cells capable of a long cyclic life is a difficult problem that appears to increase as the size of the cell is increased. Although there were a number of large active efforts to evaluate the problems associated with the application of large capacity nickel cadmium cells, such as 100 ampere hour, to space stations and communication satellites, there are only a few small programs attempting to improve the cell components. It has been generally agreed however, that in order to achieve the high performance, high reliability, and long cycle life (5 years or longer) desired for space stations, a means must be found to produce a much more uniform, consistent, defect-free, and controlled product than is presently being made available by the manufacturers.

The primary objective of this program is to develop the procedures, processes and controls, and select the materials and equipment necessary to determine the production methods needed to secure uniform, consistent, and defect-free plaque material.

The body of this report deals with the means by which the objective was pursued and met. Table 1 identifies the basic materials required to fabricate plaque. Development of methods necessary to produce high quality plaque was based on characteristics of these basic materials.

Table 1

Basic Materials for Porous Nickel Plaque

Nickel powder

Binder

Alcohol

Water

Pore Former

Nickel Grid

## EXPERIMENTAL

### A. Nickel Grid

A contractual requirement was that the grid be nickel and that the plates have an integral tab. The grid selected was of 3 mil nickel, alloy 200, perforated with a square array of holes having diameters 0.045 inch on 0.066 inch centers. The open area calculated is 37%, but a weight determination indicated that the open area is 40%. The three mil grid is preferred over 5 mil stock which was also considered. The thinner stock has sufficient strength for the process as developed and yields a better ratio of void volume to nonactive mass. The importance of void volume will be discussed more fully later.

The weight of the 3 mil grid material used is  $40.7 \text{ mg/cm}^2$  which may be compared to  $36.6 \text{ mg/cm}^2$  for nickel wire screen having 7 mil wire and a 20 x 20 mesh. Wire mesh is difficult to make flat, place into the center of plaque and also has a propensity for short circuiting by protruding wires. The last comment precludes its use as being incompatible with highly reliable cells unless special steps are taken to overcome the problem.

As received the unperforated portions of the grid are still soft annealed, while the perforated portion has been stretched and is work-hardened by the perforation process. This condition results in plaque that is not flat. To overcome this problem the material is stretched to equalize the work hardening.

In order to stretch the grid material the grid is cut into 100 foot lengths and the ends soldered around a pipe. One end is secured to a stanchion and the other end pulled to just beyond the yield point. Stretching is continued until a permanent elongation of 0.25% (3 inches) is achieved. The grid material is now flat and is rolled up on a drum after disposing of the two soldered ends. For larger volume needs, an

automatic work hardening process could be readily substituted for the manual process just described.

The grid is next cleansed. The apparatus used is shown in Figure 1. It is a stainless steel tub having two rollers, and is facilitated for heating. The grid is mounted on one roller. The tub is filled partly with trichloroethylene and the grid rolled through at 1 foot per minute. Next an alkaline cleanser is used (MacDermid Metalex-W-Special). Concentration is 6 ounces of cleaner per gallon of solution which is heated to 60°C. The grid is rolled through the solution at 1 foot per minute and then rinsed with a deionized water spray. Following this procedure water adherence to the grid is uniform.

The final cleansing step is made with a 3.3% hydrogen peroxide solution brought to pH 11 or higher with ammonium hydroxide.<sup>(1)</sup> The solution is heated to 70°C and the grid rolled through at 1 foot per minute. The grid is then washed and dried using hot air. Once cleaned the grid will hold a film of water without breaking for at least 15 seconds.

The two processes previously described, that of stretching and work hardening and cleaning, are responsible for flat plaques that preclude air entrapment during slurry application and also improve adhesion of sinter to the nickel grid. At this point the grid is ready for coating.

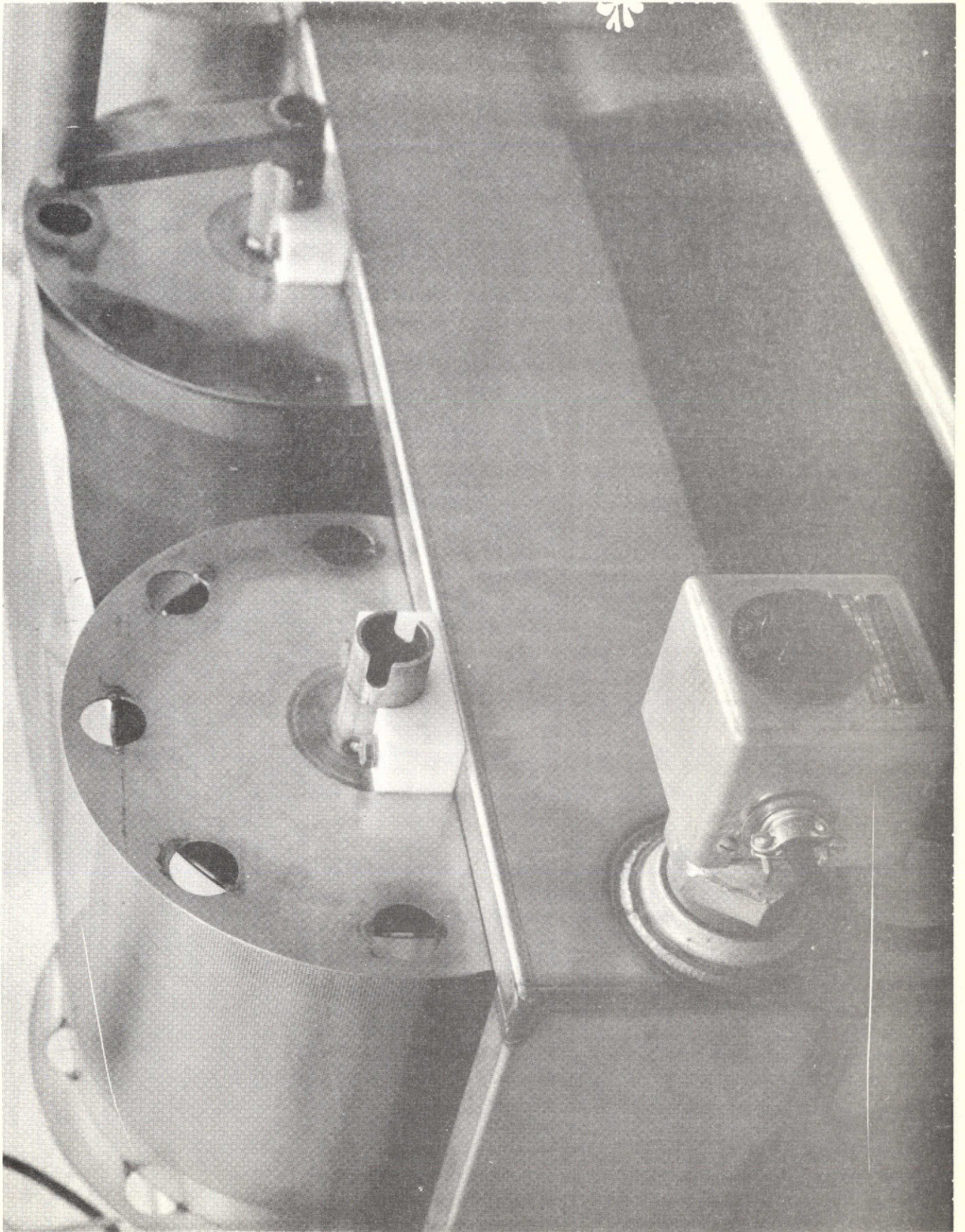
#### B. Pore Former

The active materials present in plates undergo density changes during charge and discharge. This is especially severe in the case of the positive electrodes because the active material is aggregated on the walls of the interstices. Discharging appears to stress the welded particles. To resist

---

(1) D. O. Feder and D. E. Koontz, Symposium on Cleaning of Electronic Device Components and Materials, ASTM Special Technical Publication 246, p. 40, 1959.





ORIGINAL PAGE IS  
OF POOR QUALITY

Figure 1. Grid Cleaning Apparatus



these stress conditions a strong sinter is required. Strong sinters can be achieved by using high sintering temperatures, but high sintering temperatures decrease porosity.

There are two simple approaches to achieving strong sinters without sacrificing porosity. One is to use a carbonyl powder of smaller needle size, and the other approach is to use a pore former. There appears to be more ability to control the process with a pore former.

Pore formers, or fugatives, are not new in sintering processes. Camphor, sawdust, flour, and ammonium carbonate have been used in the dry powder plaque production processes, while sawdust and flour have been employed in wet slurry plaque processes. There is alcohol in some slurries that precludes the use of camphor, and ammonium carbonate is water soluble. Sawdust and flour swell in water and are not of controlled size. Flour and sawdust also yield a large amount of carbon as a residue and become unsuitable from that point of view.

It had been decided that the slurry method was preferred over the dry powder method. There are two reasons for this choice. The first is uniformity--nickel powder has poor flow characteristics and as a result a uniform surface has just not been obtained over large areas. The second reason is that the utilization of positive active material had been found to be 120% in this laboratory on purchased slurry-processed plaque compared to 105% for purchased loose-powder processed plaque.

None of the pore formers mentioned earlier meet the requirements for use in slurry process containing both alcohol and water. A literature search revealed only one potential pore former which is oxamide ( $\text{H}_2\text{N OC-CO NH}_2$ ). Oxamide is but slightly soluble in water, insoluble in alcohol, decomposes into gaseous products at  $419^\circ\text{C}$ , is relatively inexpensive and is readily sieved to obtain a suitable particle size. The residue from pyrolysis in the reducing atmosphere furnace is 0.2%.

Oxamide is the material selected as a pore former. It is sieved through a 200 mesh screen prior to adding it to the slurry mix.

C. Binders

A total of 6 binders were investigated in this program. These were namely:

Pluoronic 127

Klucel

Carboxy methyl cellulose (CMC)

Methocel 400

Methocel 1500

Polyox

Pluoronic makes water thixotropic, but the concentration needed was 20% to achieve this situation and was ruled out. At a 20% level, costs are high, handling difficult and residue is excessive. Klucel and CMC allowed the slurry to settle out too rapidly while Methocel 1500 and Polyox exhibited good settling characteristics. Polyox however, can be deaerated more readily and has good mixing properties. The good mixing characteristics are imparted by the dispersion of the material in alcohol and its subsequent dissolution in water. The selection of binder was polyox, but either methocel could be readily substituted. It is easier to disperse and dissolve polyox which is done at room temperature, than to cool and later heat the methocel materials.

Polyox must be mixed with special precautions because it undergoes shear degradation and precipitates out of hot solutions. The precipitation results in a loss of its binding ability. When green plaque was dried above 70°C, the nickel powder fell off the grid. Because of this phenomenon it was found that drying of the slurry must be carried out below 70°C.

The green plaque once dried at room ambient temperature is fairly supple and need not be fired immediately. This "handlability" is apparently of long duration. Instead of drying at a low temperature, however, one might consider applying the slurry to only one side of the grid and drying more rapidly. There are advantages to this latter technique when considering cell designs other than flat plate.

One might note that the loss of binding ability or recrystallization would occur in the furnace at some point. At this point the green plaque must be in a metastable state. Further consideration reveals analogous situations regardless of the binder because pyrolysis occurs at lower temperatures than nickel sintering.

#### D. Slurry Composition

The volume of slurry applied per unit area of grid is a function of doctor blade spacing, viscosity of the slurry and the density of nickel powder in the slurry. A literature search and preliminary experiments indicated that a nickel powder content of about 60% is a workable level.

The viscosity is determined by the content of the binder, the way it is mixed, the way the slurry is handled, and by the total composition of the slurry. The water content and nickel content are particularly sensitive to composition. A 1% change in water content makes a dramatic change in viscosity.

Based upon early findings on purchased plaque, targets had been set up for sinter porosities. These were 75% for positive plaque and 78% for plaque used for the negative electrode. To attain these porosities in well-sintered plaque two different slurry compositions were developed. These are given in Table 2.

Recent evidence appears to indicate that utilization of active material is a function of the porosity of plaque. Preliminary calcu-



Table 1A

## Slurry Compositions for Plaque

Material	Positive Plaque, Weight of Material, grams	Negative Plaque, Weight of Material, grams
Binder	160	165
Methanol	592	600
Water	2630	2700
Ni Powder	4800	4750
Fugative	64	445
% Comp. Ni	58.2	53.7

lations suggest that a sinter porosity of 78% will maximize capacity per unit loading. Thus, the compositions indicated which were used to fabricate plaque and cells therefrom, can be subject to improvement. The basis for these statements are given in the Appendix.

## E. Mixing

The subject of mixing the slurry is indeed important. Not only are the materials to be dispersed uniformly without agglomeration, but the characteristic of the materials must remain unchanged, and the mixture must be free of air bubbles.

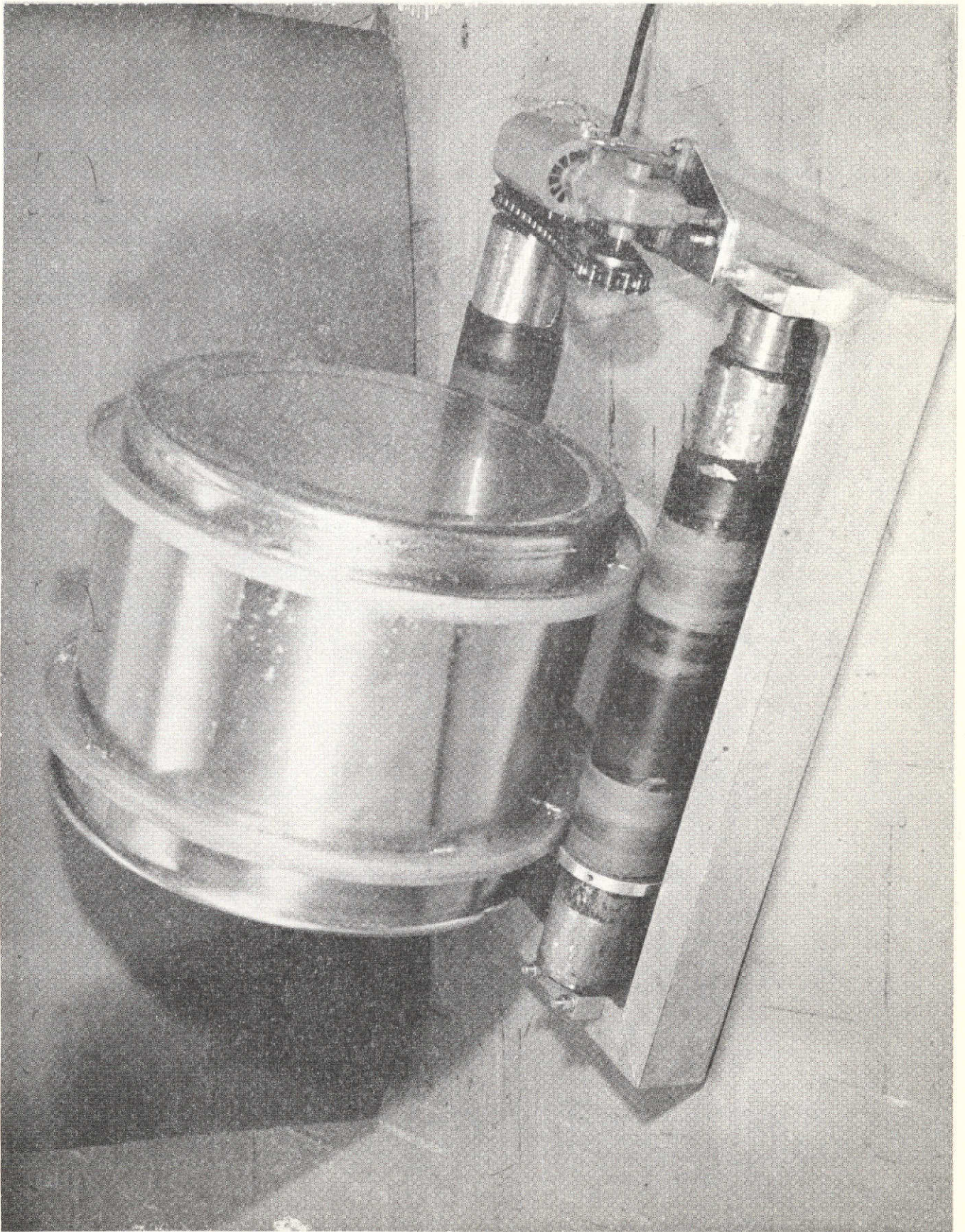
The nickel powder and the binder are both affected by shear forces. The nickel crystals break and change particle size, while shearing reduces the molecular weight of the binder used.

The slurry is started by dispersing the binder in methanol. These are stirred magnetically until the powder is completely wetted and well dispersed. The alcoholic dispersion is then slowly added to water with rapid stirring. As the mixture thickens, the stirring speed is diminished. The mixture is allowed to rest and thicken for another hour before its viscosity is measured.

The nickel powder and the pore former are blended into the water-alcohol-binder solution. These are blended until both powders are wetted. This mixing step is carried out in a stainless steel roller drum shown in Figure 2. The drum is then sealed and rolled at 0.2 to 1 RPM for 16 to 24 hours. The viscosity is then measured and adjusted to  $200,000 \pm 50,000$  cps (Brookfield Helipath TC spindle at 2.5 RPM). The drum is never filled to more than 2/3 capacity.

The slow rolling is not a uniform rolling. As the viscous material rises up the wall of the drum, the torque applies a back force which slows down the rotation. A layer of slurry then rolls over the bulk of the slurry, and the slurry thus deaerates. The slow rolling appears to be a better method for deaeration than using a vacuum or stirring slowly. The rolling does essentially the same task as slow stirring, but on a longer time basis which allows a more complete elimination of entrapped air. The evidence for the successful deaeration lies in the macroscopic and microscopic uniformity of the plaque which is virtually free of pock marks ascribed to air bubble entrapment.





ORIGINAL PAGE IS  
OF POOR QUALITY

Figure 2. Stainless Steel Drum and Roller Bearing Mill  
for Slurry Deaeration and Homogenizing



The prepared slurry can be stored for months. Prior to use, the slurry should be rolled for several hours to ensure homogeneity, and the viscosity rechecked.

The contents of the drum are transferred to a Moyno pump shown in Figure 3. The pump pushes the slurry into the applicator bucket without mixing in air bubbles. The pumping rate is controlled by level switches in the applicator bucket. A fraction of the slurry is recirculated through the pump to ensure homogeneity of the mix and uniformity between the beginning and end of a run. In this way the use of the Moyno pump is minimized. The push type mechanism in a Moyno pump does shear both the nickel powder and the binder. For this reason the pump is used only for transfer and not for mixing. When used for mixing it is observed that the viscosity of the slurry decreases. Hence, the minimization of the use of the pump. It has been integrated into the process in such a way that its good characteristics are maximized and its poor characteristics are minimized.

#### F. Green Plaque

The green plaque is made on a grid coating apparatus shown in Figures 4 A and B. Among various methods tried during the course of the work were (1) spatulation, (2) spray coating, (3) electrostatic spraying and (4) slip casting. The slip casting process was the method of choice even though it represents no major change from processes in present use. An analysis however, was made of the objectives of the chosen process for possible improvements. As a result of the analysis the coating apparatus shown in Figure 4A was designed and fabricated.

The level of the slurry in the slurry bucket is closely controlled for it is important to maintain the proper level. To control this level a float is employed. This float is located just below the grid feed roll in Figure 4B. It operates microswitches for upper and lower limits, which in turn control a solenoid that controls slurry feed rate. The



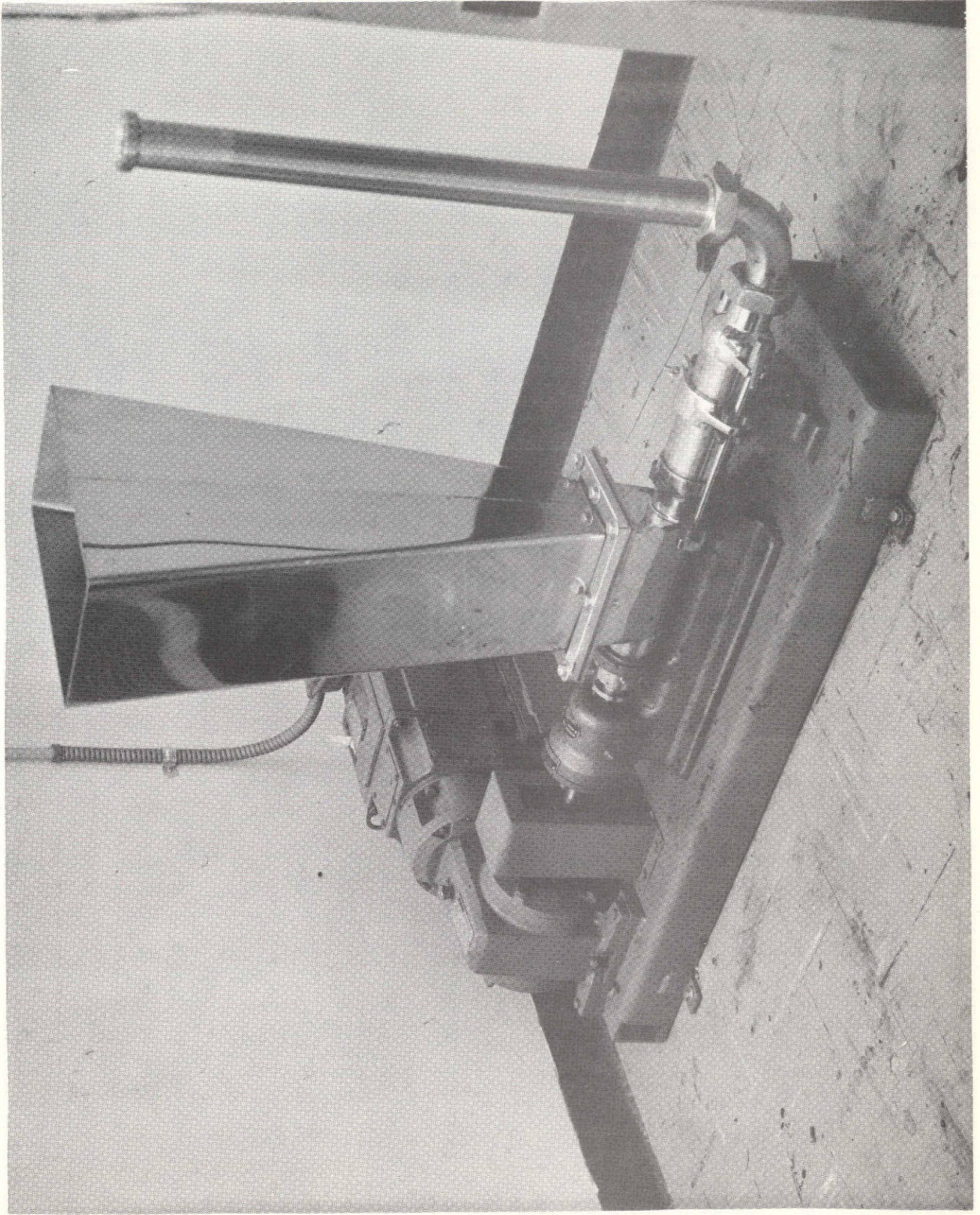


Figure 3. Moyno Pump Modified for Slurry Transfer



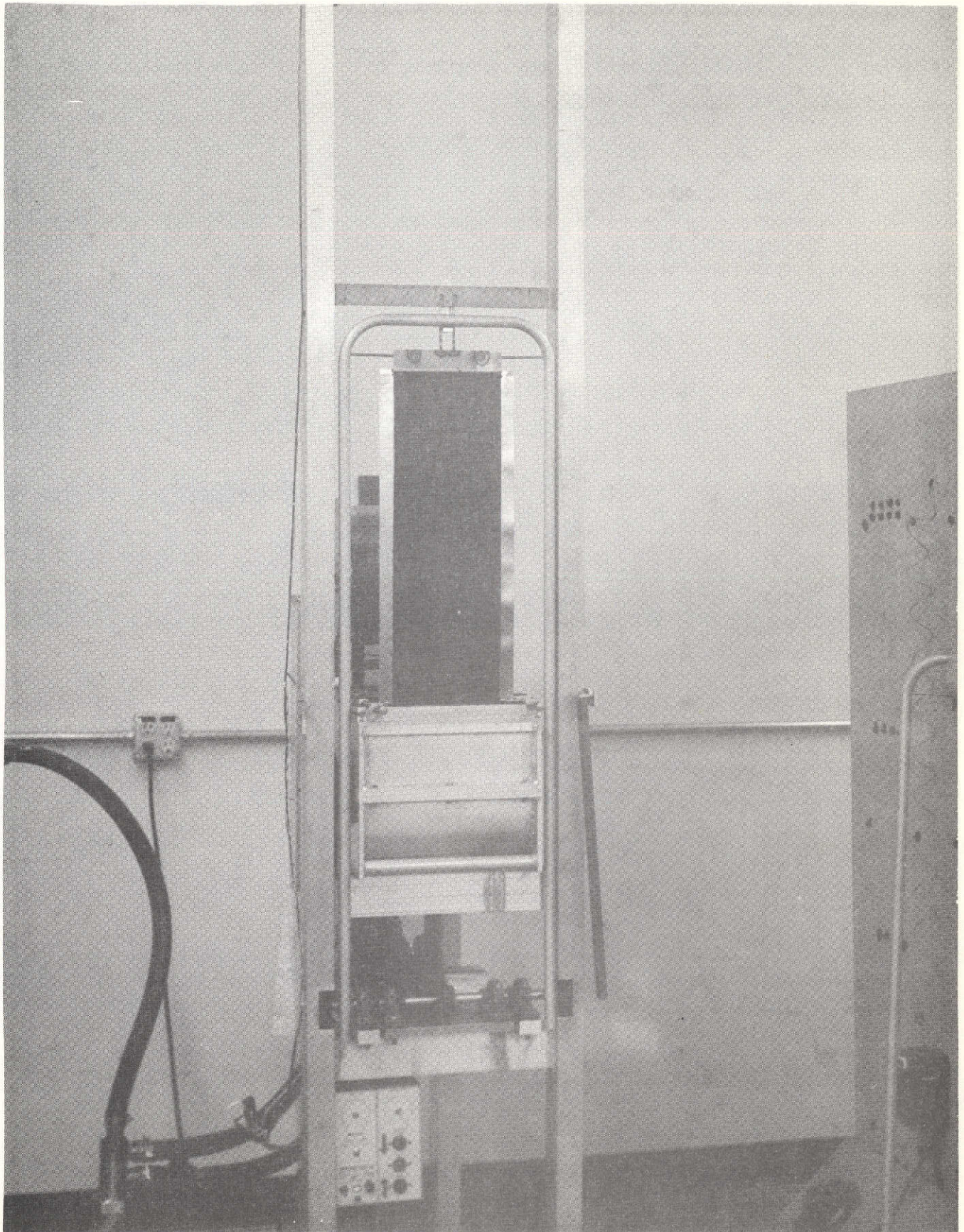
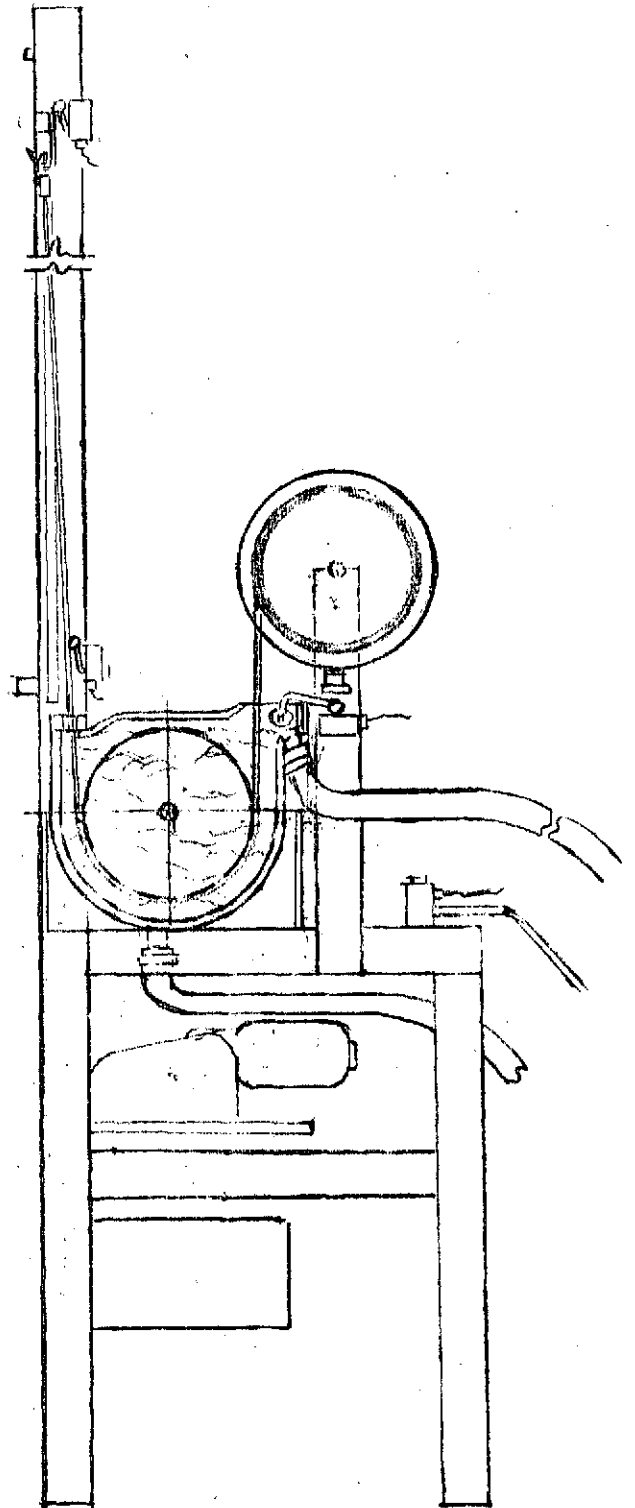
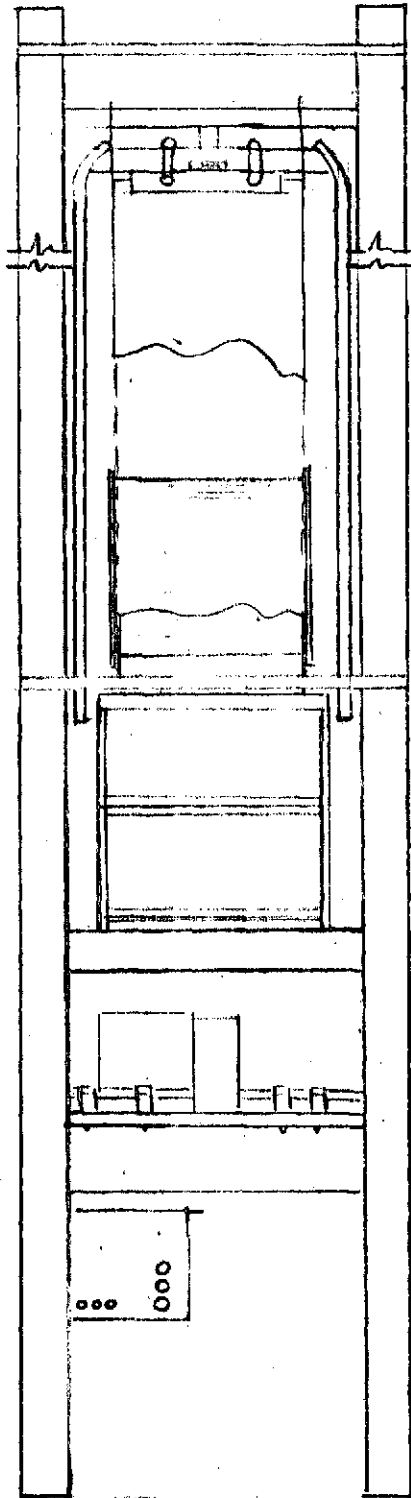


Figure 4A. Grid Coating Apparatus



ADELGADO  
DEC 31 1974

Figure 4B

ORIGINAL PAGE IS  
OF POOR QUALITY



slurry level must be controlled because it effects the amount of material placed on the grid.

The grid material, on its roller, is mounted on the machine. The grid enters the slurry slowly so that air is not entrapped. Further, the grid circles a 12 inch diameter drum immersed in the slurry. This effectively pumps slurry through the openings. The slow immersion speed avoids turbulence and aeration.

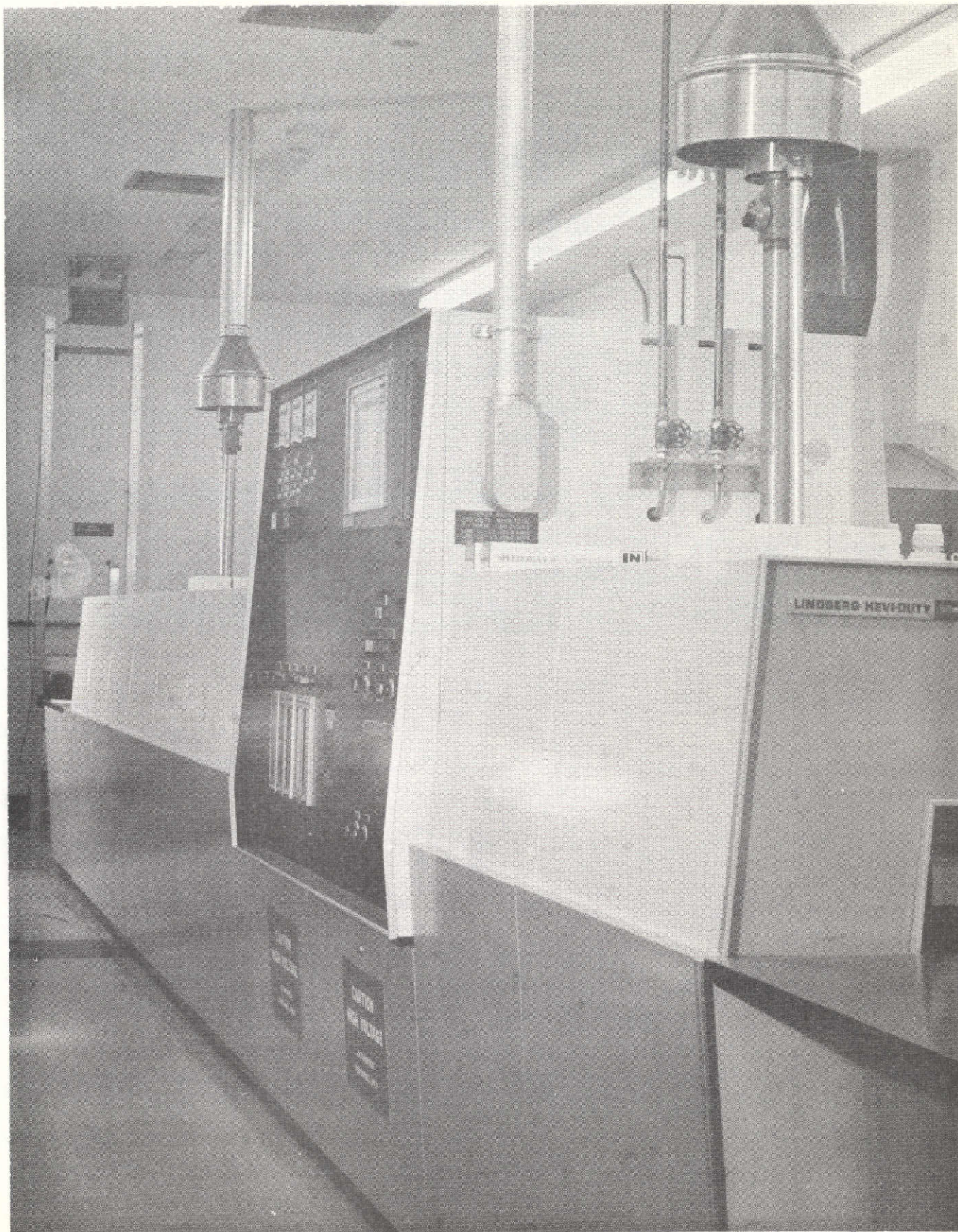
The grid material then enters the doctor blade fixture. Part of this fixture is located in the slurry, and contains teeth set at 1/2 inch intervals. The purpose of the teeth is to center the grid. The distance between the plane of the two sets of teeth is 4 mils so that the grid is centered to within  $\pm 0.5$  mils. The spacing between the doctor blades is adjustable by means of two micrometer drives. The doctor blades are parallel to within 0.5 mils to ensure uniformity of thickness. The rake angle of the blades is also important in setting plaque thickness, a rake angle of  $10^\circ$  is used which was determined empirically.

Plaque is pulled in the ascending mode by a chain drive mechanism having an extremely uniform pulling rate. The uniform pulling rate helps maintain the blemish-free and uniform characteristics. It is then allowed to dry in a vertical position below  $70^\circ\text{C}$ . The drying parameters are dictated by the binder characteristics. Once dry, the green plaque may be stored for months before sintering with only reasonable care required to avoid damage.

#### G. Sintering

The sintering furnace is conveyor belt driven in a horizontal plane as shown in Figure 5. The furnace is 28 feet long, with heating in 3 zones with 16 silicon control rectifier circuits (SCR) and two cooling zones. The belt speed is adjustable between zero and 20 inches per minute.





ORIGINAL PAGE IS  
OF POOR QUALITY

Figure 5. Horizontal Sintering Furnace with Hydrogen Atmosphere



The SCR circuits were originally designed to provide temperature uniformity. However, because of the organic binder and pore former, and the necessity of an oxidizing atmosphere region, the temperature profile at the entrance should be ramp-shaped. An actual temperature profile is shown in Figure 6. A thermocouple was imbedded into a plaque that was placed on the belt and temperature readings taken during the passage through the furnace.

The pore former used in the slurry decomposes into gaseous products at  $419^{\circ}\text{C}$ . The binder also pyrolyzes below the actual sintering temperature of  $925^{\circ}\text{C}$ . The reducing atmosphere gases are dry. To obtain a well sintered plaque some oxygen must be introduced to form an oxide monolayer on the nickel. There is, therefore, an oxidizing condition set up at the lower temperature region of the furnace. Similar processes utilize moisture and measure dew point. At elevated temperatures nickel is oxidized by water molecules. When the yet higher temperature region is reached the nickel is reduced by the dry hydrogen gas present. If sintering is carried out without an oxidizing atmosphere, the degree of sintering from the surface to the grid decreases. This results in an over-sintered surface and an undersintered region next to the grid with poor adhesion of sinter to the grid. With a proper oxidizing atmosphere the degree of sintering is strong, uniform and adhesion to the grid is strong. The oxygen flow rates and hydrogen flow rates were determined empirically. The oxygen flow rate is judged from the behavior of the gases in the furnace which is made apparent by diffraction of light. The hydrogen flow rate is next set on the behavior of the sinter as measured by electrical resistance and adhesion.

When running plaque thru the furnace, it was found necessary to place a carrier between the plaque and the steel moving belt. Where the belt links contacted the plaque blemishes occurred. These small contact areas on the plaque did not appear to be sintered to the same degree as the rest of the plaque.

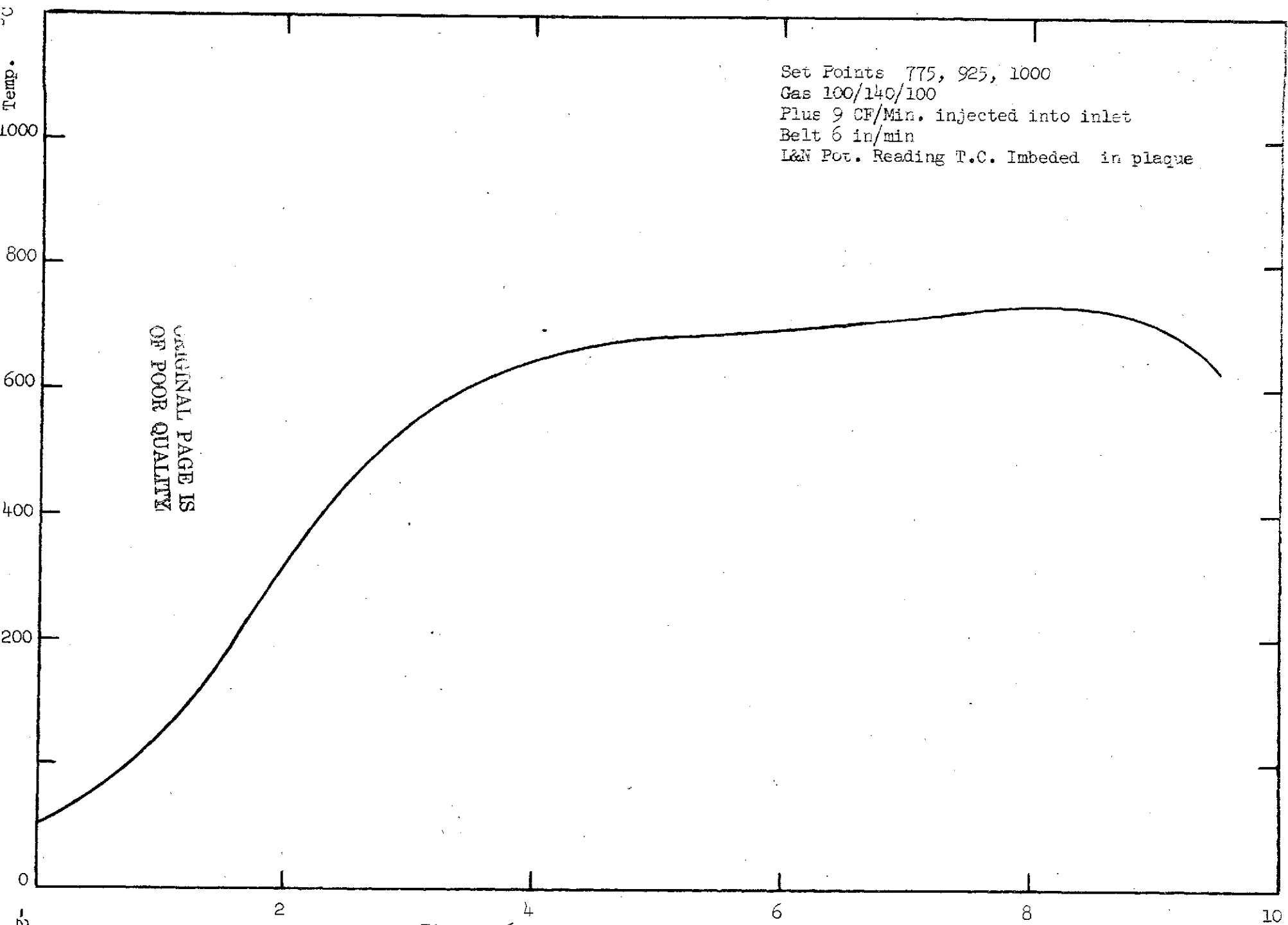


Figure -6- Temperature Profile in Sintering Furnace  
 Distance in Feet

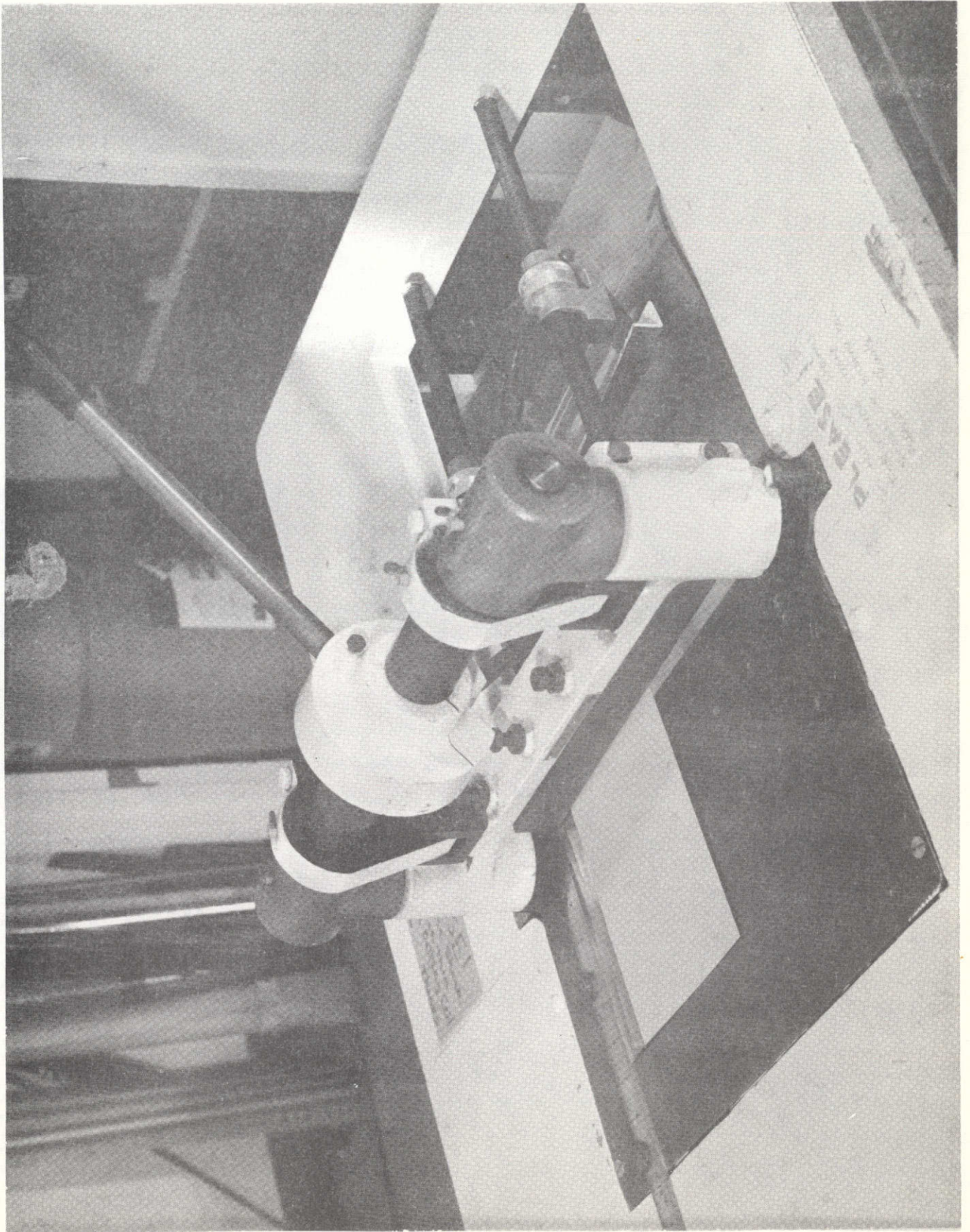
Two carriers used successfully are woven quartz fabric and inconel sheets. The material of choice is quartz. Since the thermal expansion coefficient of nickel and inconel differ, there is a "walk" of nickel with respect to the inconel which leaves surface blemishes when long sheets are used. Since these blemishes do not look well, inconel is used only for small plaques where "walk" is minimal and the cosmetic blemishes do not appear.

Upon emergence from the furnace the plaque is cut to the desired length on a shears mounted at the exit, Figure 7. Samples of plaque are set aside for measurement. Plaques are boxed and coded to correspond to the samples. The tests run for quality assurance purposes are:

1. Appearance
2. Thickness
3. Weight per unit area
4. Void volume
5. Electrical resistance.

These tests were selected from a larger group which included (a) mechanical strength, (b) grid location, (c) double layer capacitance and (d) ability to be impregnated. The test procedures are described in the following section.





ORIGINAL PAGE IS  
OF POOR QUALITY

Figure 7. Plaque Cutting Shears at Furnace Exit

## TEST PROCEDURES

### A. Void Volume and Porosity of Sintered Plaque

The capacity of a cell is dependent upon the total void volume of plaque, the impregnation level and the utilization of active material. This simplified statement may be written as:

$$(1) C = \nu L\epsilon,$$

where the definition of the symbols are obvious. This simplified equation can be regarded as exact under certain experimental conditions. One such set of conditions is an early, flooded cycle such as the final formation discharge. The utilization,  $\epsilon$ , under these conditions ranges from about 0.9 to 1.25, depending upon plaque characteristics and additives.

While the exact capacity of a cell is related to the capacity of equation 1, the importance of the uniformity of loading with active materials and of uniformity of void volume is also of utmost importance, particularly where the impregnation is carried out using an immersion process.

There are several ways to measure void volume. The most direct is to fill the voids with a liquid and determine the quantity of liquid imbibed. This is a direct measure of voids penetrated by that liquid. If the impregnation solution reaches the same voids, then the measurement is extremely useful. It has been demonstrated that approximately 95% of the voids measured by water imbibition are entered by the positive impregnation solution and converted to  $\text{Ni}(\text{OH})_2$ . In addition, this type of measurement can be reproduced to better than 2 percentile units.



The water imbibition procedure for freshly sintered plaque is:

- (a) Weigh plaque
- (b) Immerse in water
- (c) Remove excess water by dragging over glass until only microdroplets are left on the glass
- (d) Reweigh

The void volume is then calculated from the weight gain.

There is an alternative way of measuring void volume using the sample weight and geometry, but this will contain two errors. One is in the averaging to obtain thickness, and the second is in defining the surface of a plaque based on a mesh grid.

Once void volume is known, these values may be converted to porosity. Restricting void volume to the direct measurement, there remains two definitions of porosity. The first definition is plaque porosity which may be defined mathematically as:

$$(2) \quad p_p = \frac{v}{v + m/\rho} ,$$

where  $m$  is weight of the plaque,  $\rho$  is  $8.9\text{g/cm}^3$ , the density of nickel, and  $v$  is void volume. The second definition is that of sinter porosity which excludes the grid and is defined as:

$$(3) \quad p_s = \frac{v}{v + (m-g)/\rho} ,$$

where  $g$  is the weight of the grid. Two typical grid weights are  $36.6\text{ mg/cm}^2$  for 20 x 20 mesh 7 mil Ni wire and  $40.7\text{ mg/cm}^2$  for 3 mil perforated Ni, 40% open area. There is a preference for using sinter porosity, since this is related to the same kind of sinter regardless of plaque thickness.



Sinter porosity is a design parameter than enables one to obtain the same sinter characteristics for plaques of different thicknesses. Void volume is the quality assurance parameter to help ensure uniform capacity.

#### B. Thickness and Uniformity

The definition of the thickness of a plaque was brought into question while discussing void volume determination. This was brought about by the realization that plaque thickness over the grid openings is less than contiguous regions. For the purpose of cell design the definition of thickness is less ambiguous. The thickness one measures with a micrometer touching, but not compressing the material is the definition. Since positive plaque tends to thicken during impregnation, some vagueness remains even in this definition.

Uniformity is the repeatability of the measurement over the sample, and from sample to sample. Uniformity in this work is given as the variability:

$$(4) \quad v = \frac{\sigma}{\bar{X}} \times 100,$$

where  $\sigma$  is the standard deviation from the mean,  $\bar{X}$  is the mean and  $v$  (variability) is expressed as a percentage.

#### C. Grid Location

It had been intended to measure the depth at which the grid is located by scraping the sinter on a sample and using a depth gauge. However, the doctor blade fixture design adopted centers the grid so well that the value of such measurements are trivial.

#### D. Mechanical Strength

The desire was to sinter plaques in such a way as to resist blistering and shedding. Part of this problem is due to the hydrated oxides formed on conversion, and part is due to plaque that is not sufficiently strong to resist the pressures built up within the voids.

At the beginning of this program, before the grid centering was solved, an analysis was run on plaque by analogy to a reinforced concrete beam.<sup>(2)</sup> Because the neutral axis was dependent upon the location of the grid, and the strength measured could differ by a factor of 4 in a 25 mil thick plaque, the 4 point bend test was not used.

The real measurement would be resistance to a volume change within the interstices of the plaque. Bell Telephone Laboratories<sup>(3)</sup> impregnates a plaque with water and then plunges the wet plaque into liquid nitrogen. This test is quantitative at the one pressure corresponding to the volume change from water to ice.

A coining test was decided upon although it is unidirectional as is the 4 point bend test. A device was built, Figure 8, with which a 25 pound weight is lowered onto the plaque. The coining stud has a diameter of 0.088 inches resulting in a pressure of 2 tons per square inch. Results are obtained quickly and repeatably. Orientation of the face does not affect results. There are differences in results between operators which probably could be eliminated by automating the device.

- 
- (2) S. Timoshenko, Strength of Materials, D. Van Nostrand, Princeton, 1962  
(3) Private Communication from Dr. R. Beauchamp



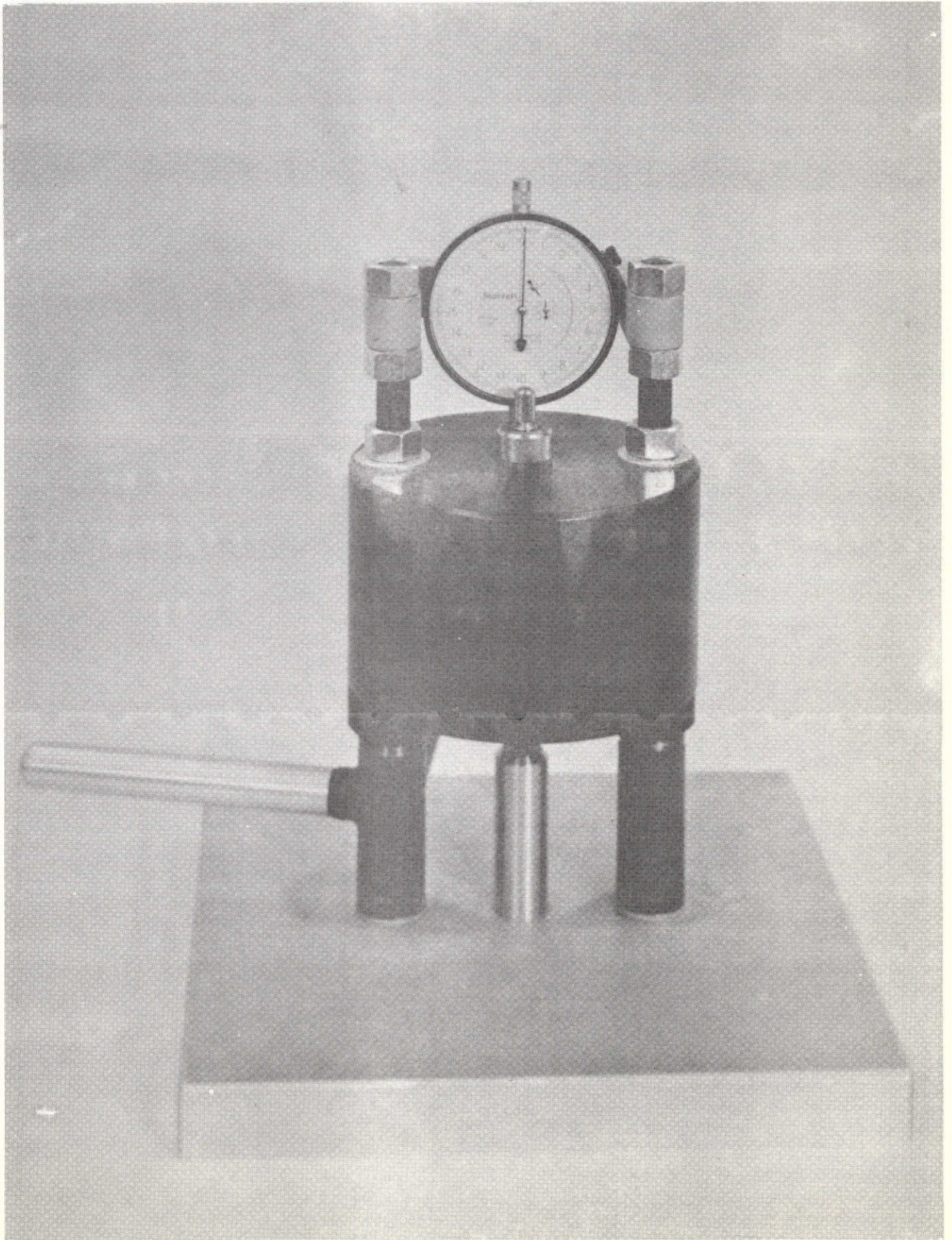


Figure 8. Plaque Hardness Testing Apparatus



### E. Plaque Surface Area

The surface area in batteries has been suspected of being important, but this has not been established. One reason, perhaps, for the lack of correlation has been the use of gaseous measurements of surface area. Gases with their low molecular weights and surface tension can penetrate regions inaccessible to electrolyte. This consideration leads to the necessity of measuring only the area represented by the electrode/electrolyte interface. In turn this suggests measurement of the double layer capacitance.

The double layer capacitance is most usually measured by impressing a current and measuring  $dv/dt$ . The voltage usually changes by a significant amount due to faradaic processes which should be avoided as much as possible because the slope  $dV/dt$  is not then indicative of the charge placed on the double layer.

If instead of a current, a voltage step is impressed and the voltage step is small enough to preclude major faradaic processes, then the differential double layer capacitance could be measured by integrating current required to reach a steady voltage state at the impressed potential.

Consider an unpoised electrode with a double layer in existence at the interface. A potential  $V_0$  will be exhibited due to a double layer charge  $q_0$ . The capacitance then is given by the equation:

$$(5) \quad V_0 = q_0/C.$$

When a small additional voltage is applied to this electrode, and it is assumed that this appears only across the electrode/electrolyte interface, a current will flow. The current will charge the interface. If the faradaic and thermal reactions are minimized the current will decay to zero, and the voltage-charge relation may be written as:

$$(6) \quad V = \frac{1}{C} (q_0 + q),$$

where  $V$  is the new electrode potential and  $q$  is the additional charge placed on the double layer. If the two sets of quiescent conditions are subtracted, and one defines  $\eta = V - V_0$ , then:

$$(7) \quad \eta = \frac{1}{C} q, \text{ or}$$

$$(7a) \quad C = \frac{1}{\eta} \int_{t=0}^{t=\infty} i(t) dt .$$

Equation 7a is used both for calculating the double layer capacitance as well as for testing for errors due to faradaic currents. Equation 7a is similar to that used by Bird, et. al.<sup>(4)</sup> A second test for absence of faradaic currents is a plot of  $\eta$  versus peak current which should be proportional. Yet a third test is that the current reaches zero. A fourth test is: after removing the applied potential and the electrode returns to its original value, the current must correspond to removal of charge from the double layer and the charge removed must equal to charge injected into the capacitor. Because unimpregnated plaque is an unpoised electrode the last test must be applied judiciously using the actual rest potential at the time the capacitative discharge current reaches zero.

The test cell used to measure double layer capacitance is shown in Figure 9. A three electrode system is used. It is important that the counter electrode is spaced from the test electrode sufficiently to preclude evolved gases from reaching the test electrode. In these experiments a nickel oxide electrode was used as a reference electrode. The cell is filled with electrolyte to cover the test electrode.

The instrumentation is shown in Figure 10. An Exact Model 505B provides the pulse. Because of the limitation on pulse amplitude and the stable lower limit of the wave form generator, a voltage divider is used. The

---

(4) J. Bird, et al, Power Sources Conference Proceedings, p. 146, 1968

$\text{NiOOH}/\text{Ni}(\text{OH})_2$   
Reference Electrode

Ni Plaque  
Test Electrode

Ni Sheet  
Counter Electrode

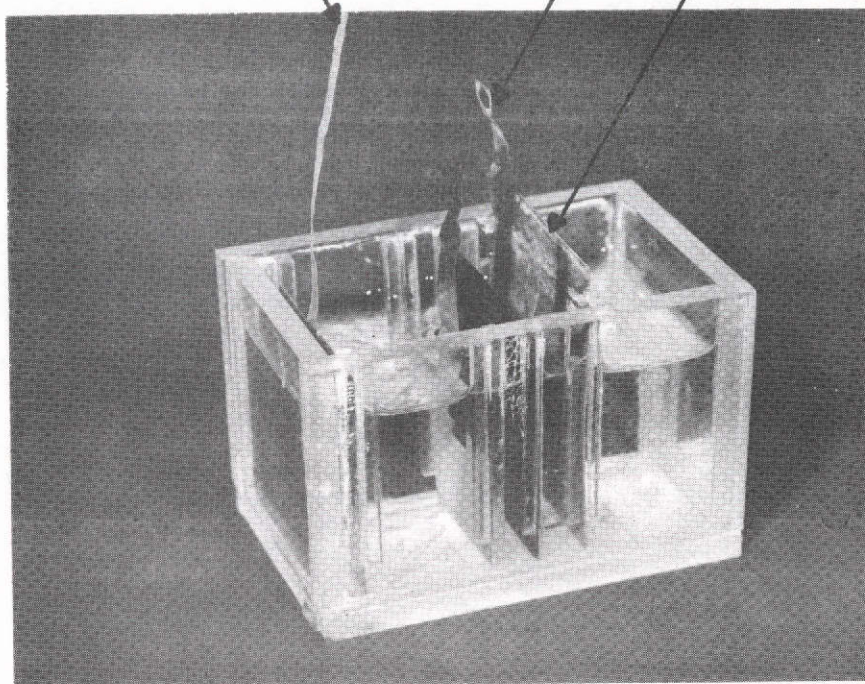


Figure 9. A Test Cell for Double Layer Capacitance Measurements

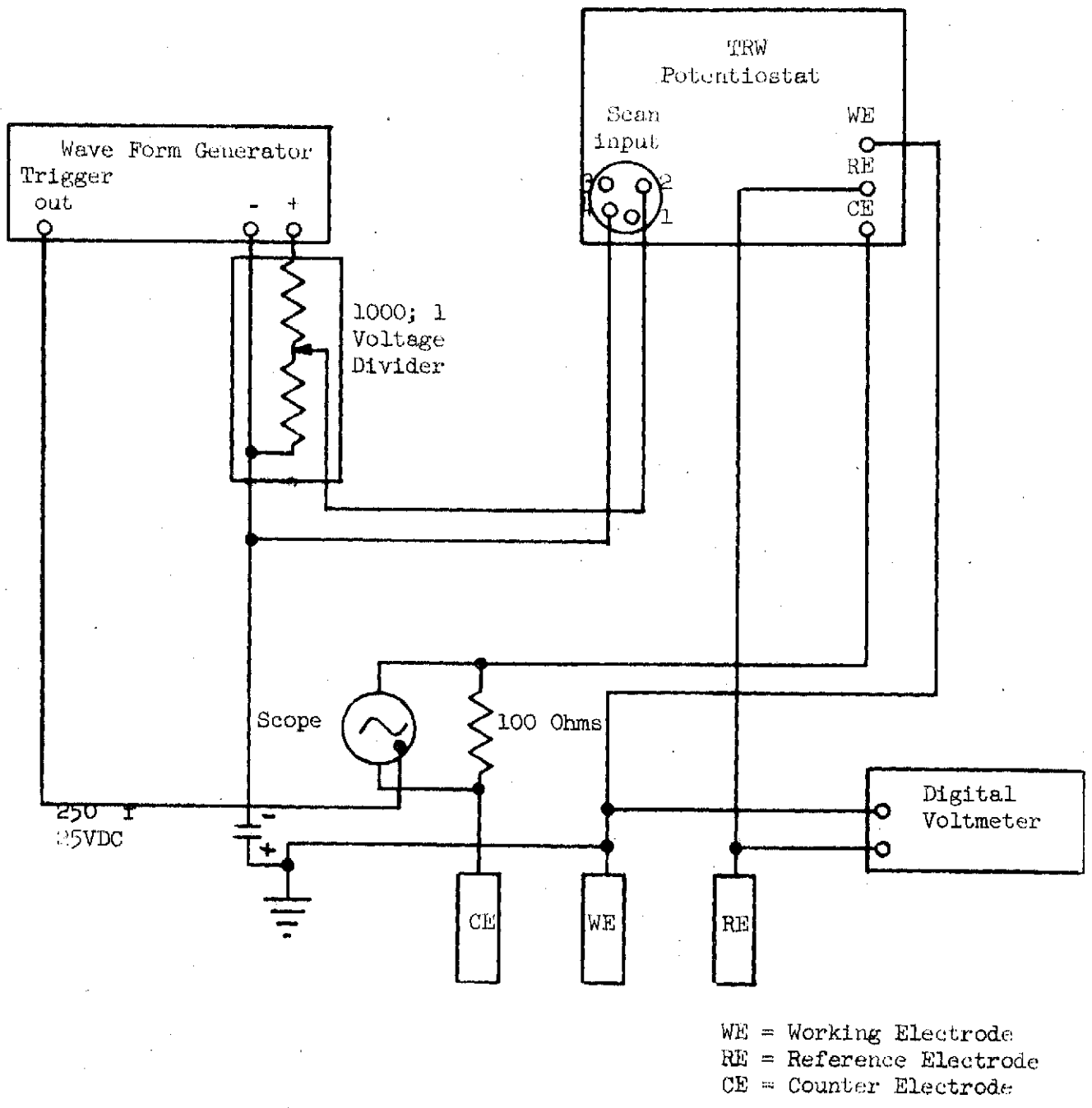


FIGURE 10: A EXPERIMENTAL SET-UP FOR VOLTAGE STEP MEASUREMENTS

ORIGINAL PAGE IS  
OF POOR QUALITY

condenser indicated between the shielded case and ground is a filter. The output of the generator is the input to the TRW Potentiostat. The current is measured as the voltage drop across a 100 ohm resistor in the counter electrode leg of the circuit. The digital voltmeter is used to measure the reference to test electrode potential.

The unpoised electrodes exhibit potentials about 800 mV cathodic to the reference electrode. Figure 11 is an example of data taken on a plaque biased over a range of potentials. The potentiostat sets the bias. The pulse from the wave form generator then is superimposed on the biasing setting and the current through the resistor is displayed on the oscilloscope. It is obvious that faradaic currents may be neglected in potential ranges of 600 to 900 mV cathodic, but at more anodic potentials accurate double layer capacities could not be determine. With the test plaque at 700 mV, near the unpoised potential the integrated charge curves are proportional to the amplitude of the voltage pulse provided that the amplitude does not exceed 15 mV, Figure 12. The capacitative charging current reaches zero about 15 ms after the pulse is impressed. The peak currents are indeed directly proportional to the pulse amplitude as shown in Figure 13. Thus the data satisfy two requirements to prove that faradaic current is inconsequential. At pulse amplitudes greater than 15 mV, the slope changes.

Once the area under the curve is obtained, the double layer capacitance is calculated using equation 7a. The double layer capacitance of smooth nickel is taken as  $20 \mu\text{f}/\text{cm}^2$ .<sup>(5)</sup> Using this value the surface area of the electrode/electrolyte interface is calculated.

#### F. Electric Resistance

The electrical resistance of plaque is expected to be a measure of the quality of the sintering process. A complication involved is the presence of the grid. The plaque resistance can be measured either from

---

(5) A. C. Makrides, J. Electrochem. Soc., 109, 977 (1962).



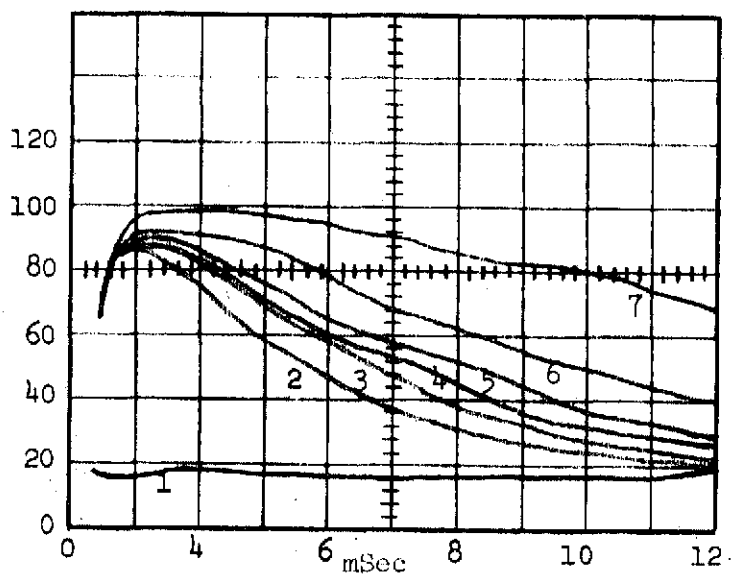


Figure 11. Current Versus Time Behavior as a Function of Biased Pulse Base Potentials, Voltage Step = 8 mV

Curves from lowest to highest	Biased Base Potentials (vs. NiOOH/Ni(OH) <sub>2</sub> )
1. Lowest	- 0.900V
	- 0.800
	- 0.700
	- 0.600
2.	- 0.500
3.	- 0.400
4.	- 0.300
5.	- 0.200
6.	- 0.100
7.	0.00

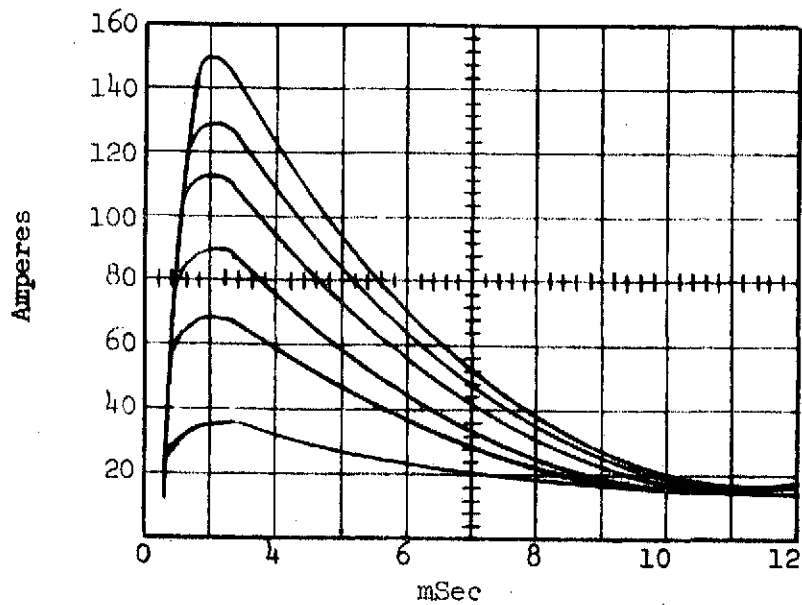


Figure 12. Current - Time Response of a Ni Plaque (Heliotek's #9) as a Function of Voltage Pulse Amplitude in a 30% KOH Solution.

Pulse Amplitudes (From bottom curve to upper curve):  
 2 mV, 6 mV, 8 mV, 11 mV, 13 mV, and 15 mV.

Base Potential of Ni Plaque = -0.700V vs. Charged NiOOH/Ni(OH)<sub>2</sub>

T.E. Base Potential  
= -0.700 V vs. NiOOH/Ni(OH)<sub>2</sub>

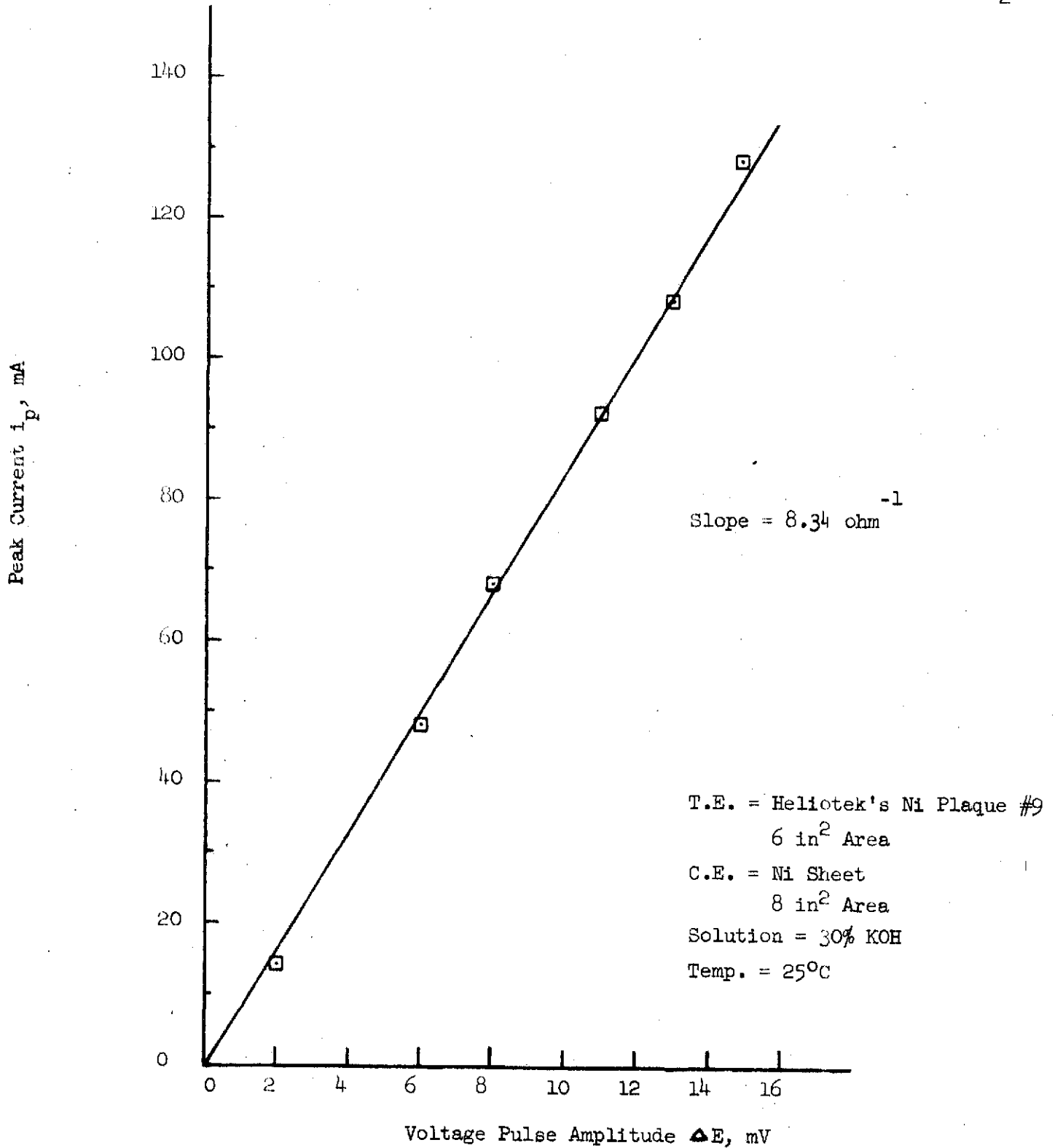


Figure 13. Peak Current  $i_p$  as a Function of Amplitude of Voltage Pulse

surface to surface or along one surface. Greater values of resistance are measured along one surface, and this method has previously been found to be valuable in assessing sintering quality.<sup>(6)</sup>

To make an absolute measure of resistance one has to be certain that the current density is uniform in the regions where the measurement is made. Relative measurements are able to be made more rapidly and more repeatably with less care. Relative measurements are made using a four-point probe. The probe is shown in Figure 14. The current contacts are indicated by I and are connected to a constant current power supply set at 5A. The probe is contacted to the plaque with current off to prevent arcing and welding. There is a shunt in the circuit to calibrate the current. The test sample is cut to 1.0" x 3.0" and the probe applied parallel to the long axis. The voltage drop is measured between the two spring-loaded pairs using a DVM.

With a 3 mil Ni sheet, alloy 200, the measured resistivity was determined to be  $11.0 \times 10^{-6}$  ohm cm. The literature value of resistivity of pure Ni is  $8.9 \times 10^{-6}$  ohm cm. To avoid confusion with absolute values of resistance or resistivity, resistance shall be reported directly as the voltage drop under the experimental conditions described.

#### G. Physical Appearance

The physical appearance of plaque is judged visually. The characteristics looked for are crazing due to mud caking during drying, pock marks and bubbles due to entrapped air. Flatness of the plaque is also gauged.

---

(6) H. N. Seiger, Unpublished data obtained between 1952 and 1956

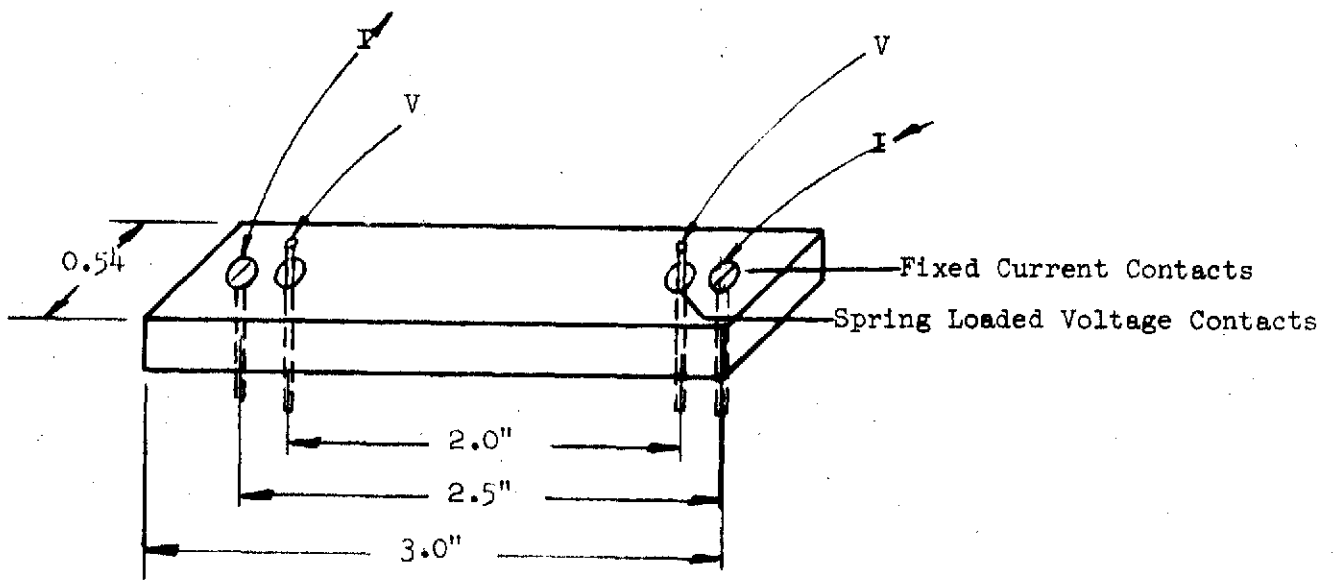


Figure 14. Multipoint Resistance Probe

## H. Impregnation Loadings

Since the prime function of plaque is to hold active materials, it is only reasonable to determine the ability of plaque to be impregnated. The more difficult plaque to impregnate to high levels is the positive plate.

Impregnations were carried out using immersion techniques. Several well known techniques were modified to assure a uniform impregnation from surface to surface, and to minimize forces on the sinter from within the interstices during conversion. These proprietary modifications minimize blisters and shedding.

## I. Scanning Electron Micrographs

The joining of nickel particles one to the other may be observed directly with a scanning electron microscope. The sintering below the surface may also be observed by breaking the plaque and looking into the region below the break. The depth of field with the method permits this to be done. SE microscopy also permits one to assess directly the sizes and distribution of the interstices.

## TEST RESULTS

The preliminary work enabled the judicious selection of sintering conditions. This included the flow rates for the various gases as well as the particular temperature profile. Calculations were made to have a target for applying slurry and sintering. It was desired to sinter plaque 25 mils thick and having a sinter porosity of 75%. These requirements set up the volume of slurry to be applied per unit area. The calculated values are given in Table 2 for negative as well as positive electrodes. These values can only approximate the geometrical attributes since plaque thickness cannot be unequivocally defined in slurry processed plaque. The thickness measured by micrometers is indicative of the number of plates that can be placed in a cell, and this measurement is important. The capacity is a function of the void volume entered by the impregnation solution. This void volume is estimated from the water imbibed. With these facts in mind, sintered plaque characteristics will be close to, but not identical with the target values given in Table 2.

The slurry composition has been given earlier. The temperature profile, the oxygen flow rate and the nitrogen curtain flow rates were previously established. The effect of furnace temperature, residence time for plaque in the furnace and hydrogen/nitrogen forming gas are variables which should be selected. A factorial experiment was run to determine the values of these variables for manufacture of positive plaque for the 100 AH cells.

Since there are only 3 factors, a two level experiment requires only 8 samples. A complete factorial was run and this also included the base level plaque conditions promulgated in the preliminary investigative work. The factorial experimental values are shown in Table 3.

Plaque was sintered and then tested. The test results are given in Table 4. Included in Table 4 are some parameters measured on plaque

Table 2

## Target Parameters for Sintered Plaque

Item	Positives	Negatives
Grid weight, gms/in <sup>2</sup>	.250	.250
Thickness, mils	25	25
Sinter porosity, %	75	78
Sinter Weight, GMS/in <sup>2</sup>	.846	.748
Plaque Weight, GMS/in <sup>2</sup>	1.096	.998
Void Volume, cm <sup>3</sup> /in <sup>2</sup>	.285	.296



Table 3

## Factorial Experiment

for

## Sintering Positive Plaque

Factor:	Furnace Setpoints °C			Belt Speed inches/minute	% H <sub>2</sub> in forming gas
	zone 1,	zone 2,	zone 3		
Base Level, B	775	925	1000	6	20
Unit change		25		2	10
High Level, H	800	950	1026	4	30
Low Level, L	750	900	975	8	10

Run No.

1	L			L	L
2	L			H	H
3	L			H	L
4	L			L	H
5	H			H	L
6	H			L	H
7	H			H	H
8	H			L	L
9	B			B	B

Table 4  
Summary of Measurements

Sample No.	Void Volume cm <sup>3</sup> /in <sup>2</sup>	Thickness mils	Mech. Strength	Surface Area cm <sup>2</sup> /gm	Electri- cal Resist. mV	Impreg. Loadings g/cm <sup>2</sup> Voids	Δ Thick. After Loading	Plaque Weight G/in <sup>2</sup>	Porosity Sinter, %
1.	.260	24.0	9.2	848	13.2	2.01	.1	1.095	73
2.	.282	24.6	9.1	990	13.1	1.99	1.2	1.170	73
3	.252	24.2	9.3	832	13.5	2.07	-.4	1.083	73
4	.291	24.9	9.6	856	13.5	1.99	1.3	1.159	74
5	.254	22.5	7.9	774	12.3	1.93	.4	1.128	72
6	.281	24.3	8.9	820	12.5	1.96	1.1	1.178	73
7	.262	23.7	8.2	808	11.7	2.02	.4	1.182	71
8	.276	22.3	7.9	804	12.9	1.96	2.8	1.145	75
9	.278	24.7	9.2	928	13.0	1.99	1.0	1.171	73
$\bar{X}$								$1.146 \frac{\sigma}{\bar{X}} = 3.2\%$	
Goal (Table 2)									
(+)	.285	25				1.99		1.096	
(-)	.296	25						.998	
No Oxid.									
ATM		29.0		528	18.0				
DA†	.271	25.2	11.5	428	21.3			.756	82
SW	.254	26.2	10.0	748	16.1			1.022	72
SF	.027	26.0	11.3	<220	13.7			.987	**
SF*	.261			994					
SA1	.225	25.0	8.9	854	21.8			.755	79
SA2	.265	30.2	10.3	835				.957	77
DB	.366	32.1	14	1022	20.8			1.024	80
SB	.346	30.8	13.1	818	10.3			1.149	**
3 Mil Ni 200					14.5				
3 Mil Perf. Grid					34.9				

\*Evacuated to eliminate entrapped air

\*\*Grid characteristics not known.

† Prefix D denotes dry powder process, while prefix S is used for slurry sinter process.

fabricated elsewhere. These plaques have various grids, and, in some instances have been made by the dry powder process.

Most of the plaque made in the factorial experiment have reached an adequate thickness and are rather strong. Electrical resistance and impregnation loading levels are also adequate. Sample No. 9 was selected for manufacture of positive electrode material. Sample No. 4 is closest to that of the negative plaque material desired. This was used as the sintering conditions and the slurry mix was altered by decreasing the quantity of nickel powder and increasing the quantity of pore former to more closely meet the targetted values.

These data can be used for analysis of the effect of the three parameters on the sintering results. To perform the analysis, the data obtained on plaque sintered at the high level of a factor were averaged and compared to the data obtained on plaques sintered at the low level. These two sets of data were examined using the student "t" test for significance. The number of degrees of freedom is 6 so that significance was taken at the 90% confidence level. The results of the data analysis are given in Table 5. The higher hydrogen flow rates are associated with an increase in void volume and thickness. The higher temperature settings increase plaque strength and conductivity while slightly, but significantly, decreases thickness. In all cases, the factors varied can be compromised without greatly varying the plaque quality. The base level, Sample No. 9, was most nearly the target values for the positives. The conditions for this sample came from the preliminary work.

Plaque was then sintered for fabrication of the 100 AH cells required by the contract. Some random samples are shown in Table 6. The plaques for the negatives are based on a 78% porosity. The last column indicates that porosity is quite uniform have a variability of 0.2%. The void volume has a variability of 3% while the specific weight has a variability of 1.5%. The process variable considered most important in impregnation by an immersion process is void volume. A variability of 3% indicates the variability that one may encounter in capacity due to void volume. The positives were targetted for a 75% porosity. The variabilities are about the same as for

Table 5

Summary of Data Analysis  
Factorial Sintering Experiment

Parameter Tested	Temperature Factor	Belt Speed Factor	Hydrogen Content Factor
Void volume	N.D.	N.D.	High level increases voids
Plaque thickness	High temperature Decreases Thickness	N.D.	N.D.
Mechanical Strength	High temperature Increases Strength	N.D.	N.D.
Surface Area	N.D.	N.D.	N.D.
Elec. Resistance	Lower Resistance at High Temperature	N.D.	N.D.
Weight Gain, G/cm <sup>3</sup> voids	N.D.	N.D.	N.D.

N.D. = No statistical significance to differences

the negative electrodes. It should be noted that a less rigorous set of sintering conditions were used for the negative electrodes to obtain greater porosity. As a consequence the resistance is greater than for the positives although the negative electrodes are somewhat thicker by about 2 mils.

Tables 6B and C contain data on the weight of plaque used for impregnation of the positive and negative electrodes for the 100 AH cells. The weight variances appear to be less for the production run than for the plaque data in Table 6A, but only because 6A represents the complete run while Tables 6B and C are for only part of the run. The weight gain variabilities are in line with the void volume variability of plaque.

The theoretical capacity of the positive electrodes in the 100 AH cell is 128 AH and of the negatives is 303AH. This ratio requires an explanation. The original impregnation processes did not load plaque uniformly. This became apparent by observing pore entry of about 65% in both positives and negatives, and by scanning electron microscopy. Work was directed to yield a uniform impregnation. The reason for the inadequate entry into the positives were found, and the process revised to effectively load 95% of the pores. The cause of non-uniform loading of the negatives is complex. While attempting to overcome the problems of the negatives, the positives were being impregnated. A reduced loading was used so that, in the event the negative plate loading could not be made uniform, there would be an adequate negative to positive ratio. Hence, the positives were loaded to a level of  $1.3 \text{ g/cm}^3$  voids instead of  $1.8 \text{ g/cm}^3$ . A partial solution was made for the negative loading and was used resulting in a loading level of  $2.2 \text{ g/cm}^3$  voids.

With further investigations completed at the end of the program, the negative loadings could be increased to  $2.8 \text{ g/cm}^3$  voids. Utilizing both improvements the theoretical capacity would be increased to 180 AH and an expected formation ratio of 1.6 to 1, negative to positive capacity.

ORIGINAL PAGE IS  
OF POOR QUALITY



Table 6A

## Plaque Processed for 100AH Cells

## Random Sample Data

Plaque Type	Thickness Mils	Void Volume cm <sup>3</sup> /in <sup>2</sup>	Weight GM/in <sup>2</sup>	Electrical Resistance MV	Sinter Porosity %
Pos.	25.4	.264	.990	12.9	76.1
	25.5	.271	1.044	12.9	75.3
	26.3	.262	1.017	12.4	75.3
	26.6	.288	1.088	12.3	75.3
	25.9	.280	1.053	12.8	75.7
Ave.	25.9	.273	1.040	12.7	75.5
Variability, %	1.9	4.3	3.6	2.1	0.5
Neg.	28.2	.314	1.011	14.9	78.6
	27.6	.301	.986	14.4	78.4
	28.5	.317	1.023	14.1	78.3
	27.9	.303	.993	15.0	78.5
	28.1	.304	.992	14.3	78.6
Ave.	28.1	.312	1.001	14.5	78.5
Variability, %	1.3	3.0	1.5	2.7	0.2

Table 6B

## Negative Electrode Impregnation Data

100 AH Batch No. 1

Plaque No.	Plaque Wt.	Weight Gain
1	46.8	31.6
5	46.3	30.3
10	46.7	29.3
14	46.4	30.5
20	46.4	32.1
25	46.5	31.0
30	46.6	29.4
35	46.4	33.4
40	46.7	31.9
45	46.3	31.3
50	46.4	32.2
55	46.3	32.7
60	46.7	33.1
65	45.7	31.1
70	46.5	34.0
75	45.6	35.4
80	46.2	33.8
85	47.8	29.7
90	47.0	32.6
95	45.8	33.6
100	47.9	33.4
105	46.7	31.3
108	<u>46.2</u>	<u>31.8</u>
	46.5	32.0
	V = 1.1%	V = 4.8%

Table 6C

## Positive Electrode Impregnation Data

100 AH Batch No. 2

Plaque No.	Plaque Wt.	Weight Gain
1	52.5	17.7
5	52.0	17.6
10	52.2	16.9
15	52.6	17.3
20	53.2	17.2
25	52.9	17.8
30	53.0	17.9
35	52.2	17.2
40	52.8	18.0
45	52.4	17.2
50	51.5	16.9
55	52.6	18.5
60	53.4	17.8
65	52.8	17.9
70	52.8	18.2
75	53.6	19.0
80	52.6	18.7
85	53.0	18.2
90	53.2	19.1
95	53.3	17.9
100	52.6	17.0
105	52.4	17.5
108	<u>53.6</u>	<u>18.4</u>
	52.8	17.8
	V = 0.9%	V = 3.4%

## 100 AH CELL DESIGN

The design features of the 100 AH cell are given in the Statement of Work (L18-1380) as:

- (a) Opposed terminals
- (b) Full width plate tabs
- (c) Integral plate tabs and substrate
- (d) Pure nickel substrates
- (e) Polypropylene separator, if found acceptable
- (f) Consideration given to thermal control

Thermal analysis <sup>(7)</sup> indicates that heat can be conducted to the cell cases via the grid. The greater the number of grids the better the conduction so that 25 mil thick electrodes were selected. One ceramic to metal seal was used in the cell and that was for the positive terminal. It is contended that corrosion processes are dependent upon the potential with respect to the electrolyte rather than on potential drops. Since the positive electrode on open circuit is about +0.5 volts to a SHE in the same electrolyte, the corrosion rate at the positive braze will be the same whether the negative plates are joined to the case or to another seal. To clarify this point, imagine a SHE appropriately equipped as a test probe in the solution. This probe is used to measure the potentials. The potential governs the processes that occur. If the probe indicates

---

(7) R. McGrath, Final Report to Heliotek, HAC Data Bank 1-4189, October 1971.

that one braze alloy is at the same potential as the positive electrode because it is short circuited to the positive by design, these certain processes can occur. These processes are (1) oxygen evolution on low overpotential braze alloys and (2) oxidation of certain metals present in the braze. Silver and copper are two materials which are oxidized at the potential of the nickel oxide electrode. If a noble metal such as platinum is present, this has a low oxygen overvoltage, and, although it will not corrode, it will decrease the charge efficiency. Hence, the double ammeter test has great value in materials selection for seals.

The braze joint short-circuited to the negative electrode is protected against corrosion. The other braze joints are at floating potentials. If any attain values close to the negative electrode then reduction can occur. Potentials at the floating braze joints will be dependent upon the composition of the gas present in the cell. Since oxygen is usually present, these braze joints will be at some intermediate potential.

Reduction of the oxidized silver somehow gives rise to the migration. Whenever migration is observed it extends from the intermediate braze joint to the one short-circuited to the positive electrode.

From the above discussion it is apparent that the use of a single ceramic to metal seal will not result in failure any more so than using two feed throughs. Using one seal also increases reliability as well as providing a path for conduction of heat to the case through the negative comb and tab assembly. Thus the single terminal design aids in thermal control.

The opposed tab design was followed. Full width tab integral with the substrate was used. There is a notch in the tabs for the stud



location. The tab and grid are Ni 200.

The footprint of the cell was selected to allow interchangeability with standard sealed 100 AH cells. The plate sizes are approximately 6.3" x 7" and are .025" thick. There are 25 positive plates and 26 negative plates per cell. The integral tabs of the negative electrodes are welded into a comb bar which, in turn, is welded to the bottom of the case. The positive tabs are welded to the comb bar which, in turn, is welded to the stud of the ceramic-to-metal feed through.

The separator used is a polypropylene, RAI P145122, heat sealed into bags and placed on the positive electrodes. The polypropylene separators are considered acceptable provided the cells are sealed without entrapped air.<sup>(8)</sup>

A teflon liner is used around the plate stack assembly. The teflon electrically insulates the negative electrodes from the case along the broad faces and facilitates insertion of the assembly into the case.

After filling with electrolyte and setting of precharge on the negative electrodes the cells were put through an electrical checkout. The cell design is given in Table X.

Discharge curve for cell S/N 1 at 50 amperes and 100 amperes is shown in Figures 15 and 16, respectively. This cell was formed in an electrolyte containing lithium hydroxide, and also is filled with a lithiated electrolyte. Lithiation depresses the voltage level slightly during discharge. Lithiation is suspected also of depressing the voltage level slightly during charge, which probably accounts for an improved charge efficiency.<sup>(9)</sup> Charge efficiency is a

---

(8) H. N. Seiger, Presentation at Battery Workshop, NASA/GSFC, 1972

(9) Private communication with Dr. R. Beauchamp, B.T.L.

TABLE X  
CELL DESIGN  
HNC 100.3

<u>Electrodes</u>	<u>Positive</u>	<u>Negative</u>
Porosity	75%	78%
Thickness, mils	25	25
Void volume		
Loading Level, g/Cm <sup>3</sup>	1.8	2.2
Utilization, %	120	88
Grid weight, mg/in <sup>2</sup>	262	262
Target Capacity, AH	150	225
Plate Area, Aspect Ratio, in.	6.3x7	6.3x7
Number plates/cell	25	26
Charge Current Density at c/10	4.5mA/in <sup>2</sup>	
Neg./Pos. Capacity Ratio	1.5	
 <u>Separator</u>		
Material	RAI P145122	
Density, Bulk	0.9	
 <u>Electrolyte</u>		
Density of KOH Soln.	34%	
Fill Level	90%	
 <u>Container</u>		
Material	304L	
Density	7.8g/cm <sup>3</sup>	
Wall Thickness	.031"	
Outside Dimensions	1.538x7.240x8.35"±.008	
 <u>Liner</u>		
Material	Teflon	
Density	2.3g/cm <sup>3</sup>	
Thickness	5 mils	

TABLE X  
CELL DESIGN

Combs

Material	Nickel 200
Density	8.9g/cm <sup>3</sup>
Thickness	.093 in
Design	Cantilever 6.250 x 1.250

Covers

Feed Throughs

Material	Nickel 200
Density	8.9g/cm <sup>3</sup>
Length	1.00 in
Diameter	0.56 in

Ceramics

Material	Alumina 96%
Density	4.0
Design	Single Ring, Compression Seal

Cover Blank

Material	304L
Density	7.8g/cm <sup>3</sup>
Thickness	.030
Openings	Single

Fill Tube

Material	304
Density	7.8g/cm <sup>3</sup>
Wall thickness	.022
Tube diameter	3/16

Tabs

Material	Nickel 200
Density	8.9g/cm <sup>3</sup>
Thickness	3 mil (integral)
Length and width	Plate length x 1 inch

TABLE X  
CELL DESIGN

Thermal Conductivity Consideration

Plate Aspect Ratio	1.11
Plate Thickness	25 mils
Inter electrode Spacing	.005"
Electrolyte Fill Level	90%



S/N 1 12-20-72  
Charge 50A x 2 hours + 10A x 18 hours  
ECOP 10 psig  
EOCV 1.42  
Discharge Current 50A  
Open Circuit Stand 1.5 Hours

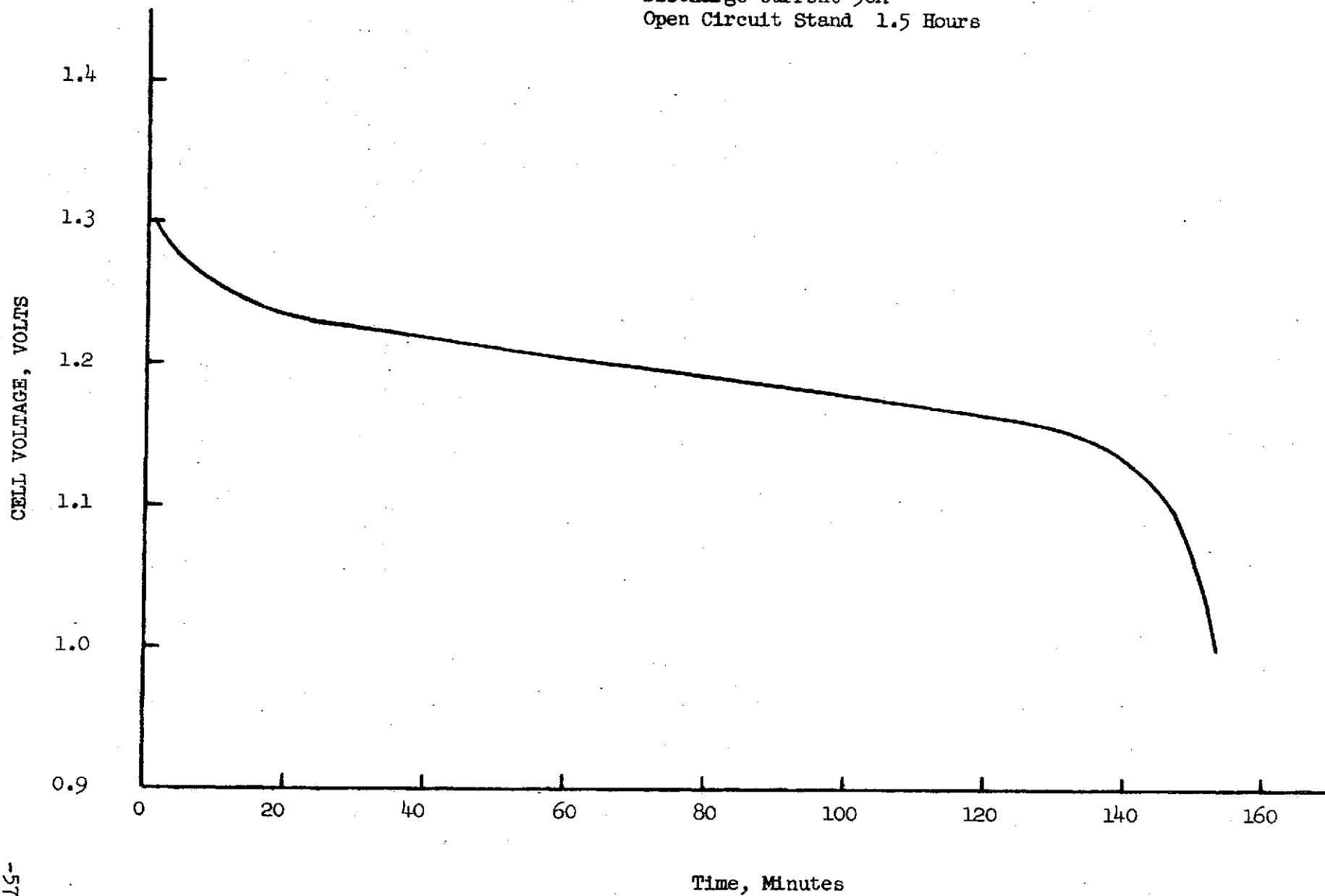


Figure -15- % Discharge Curve

S/N 1                    3-9-73  
Charge 50Ax 175 Minutes / 10Ax 160 Minutes  
EOCP 28 psig  
EOCV 1.400  
Discharge Current 100 Amperes

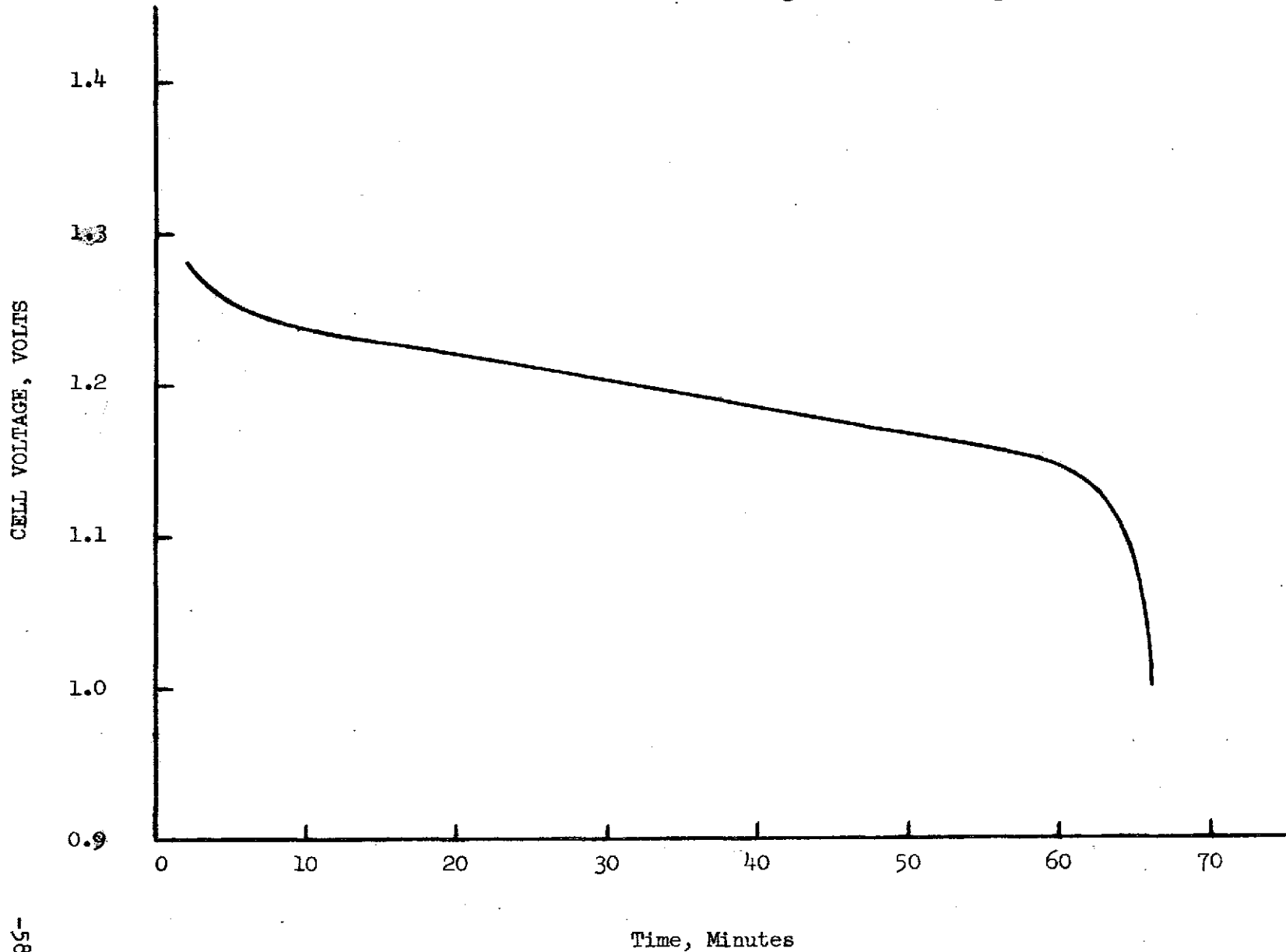


Figure -16- % Discharge Curve

function, also, of charge rate, temperature and state of charge.\* Effect of charge rate on capacity on S/N 1 is shown in Figure 17 along with previously published data.<sup>(10)</sup> Both sets of data indicate a decrease of capacity at charge current densities below  $7 \text{ mA/in}^2$  of plate area. Similar findings were also observed by MacArthur.<sup>(11)</sup>

As a result of the charge efficiency curves, it may be readily concluded that charge efficiency may be improved by using thicker plates. This will degrade the thermal transfer rate in proportion to the decreased number of plates. However, decreasing the number of plates also decreases weight and increases capacity. In the case of the 100AH cell considered here, increasing plate thickness from 25 to 33 mils decreases weight 6 ounces and increases capacity 5%.

The process of decreasing the number of plates would also decrease the total geometric area of the negative electrodes. This in turn would tend to increase the oxygen pressure during overcharge. To investigate this effect the data obtained on a 10A (C/10) charge were used to calculate the expected pressures at higher charge rates. The calculated pressure-current curve is shown in Figure 18 along with three experimental points corresponding to 15A (C/6.6) and 20A (C/5). The agreement is not as close as one might want, but it is sufficient for estimation of the pressures that may be expected when the number of plates in a cell is decreased.

It has been known that the recombination rate of oxygen at the negative electrode is greater during overcharge than while on open circuit.<sup>(12)</sup> Figure 19 shows that the recombination rate for oxygen consumption is also greater during discharge than it is on open circuit.

---

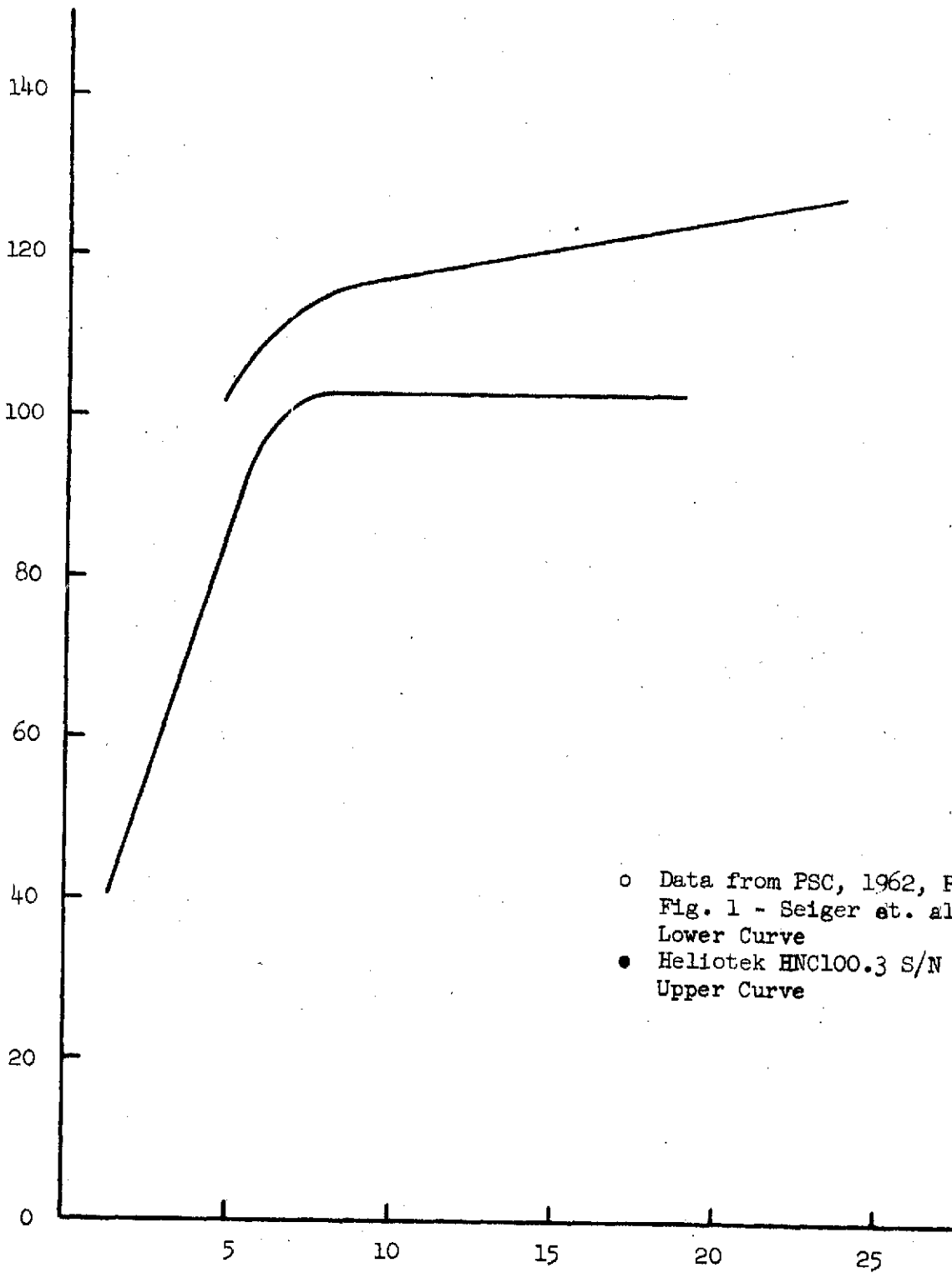
(10) H. N. Seiger, et al, Preceedings P.S.C., p. 96, 1962.

(11) D. MacArthur, Presentation at ECS Meeting, 1968

(12) H. N. Seiger, Presentation at the ECS Meeting, New York 1963

\* Charging efficiencies are also dependent on the concentration of the electrolyte.

Capacity, Percent of Cell Rating

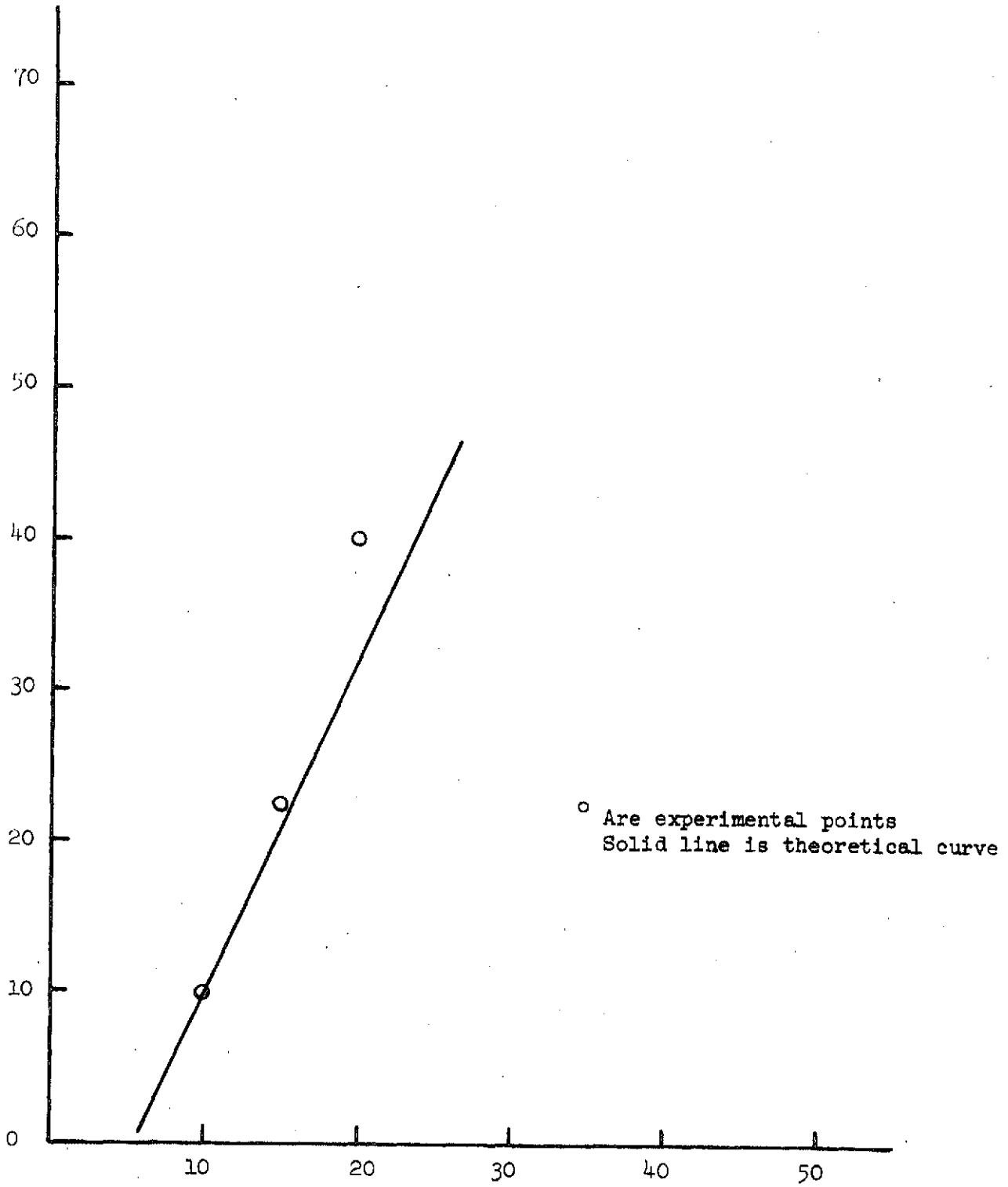


○ Data from PSC, 1962, P. 96  
Fig. 1 - Seiger et. al.  
Lower Curve  
● Heliotek HNC100.3 S/N 1  
Upper Curve

Charge Current Density, Ma/in<sup>2</sup>

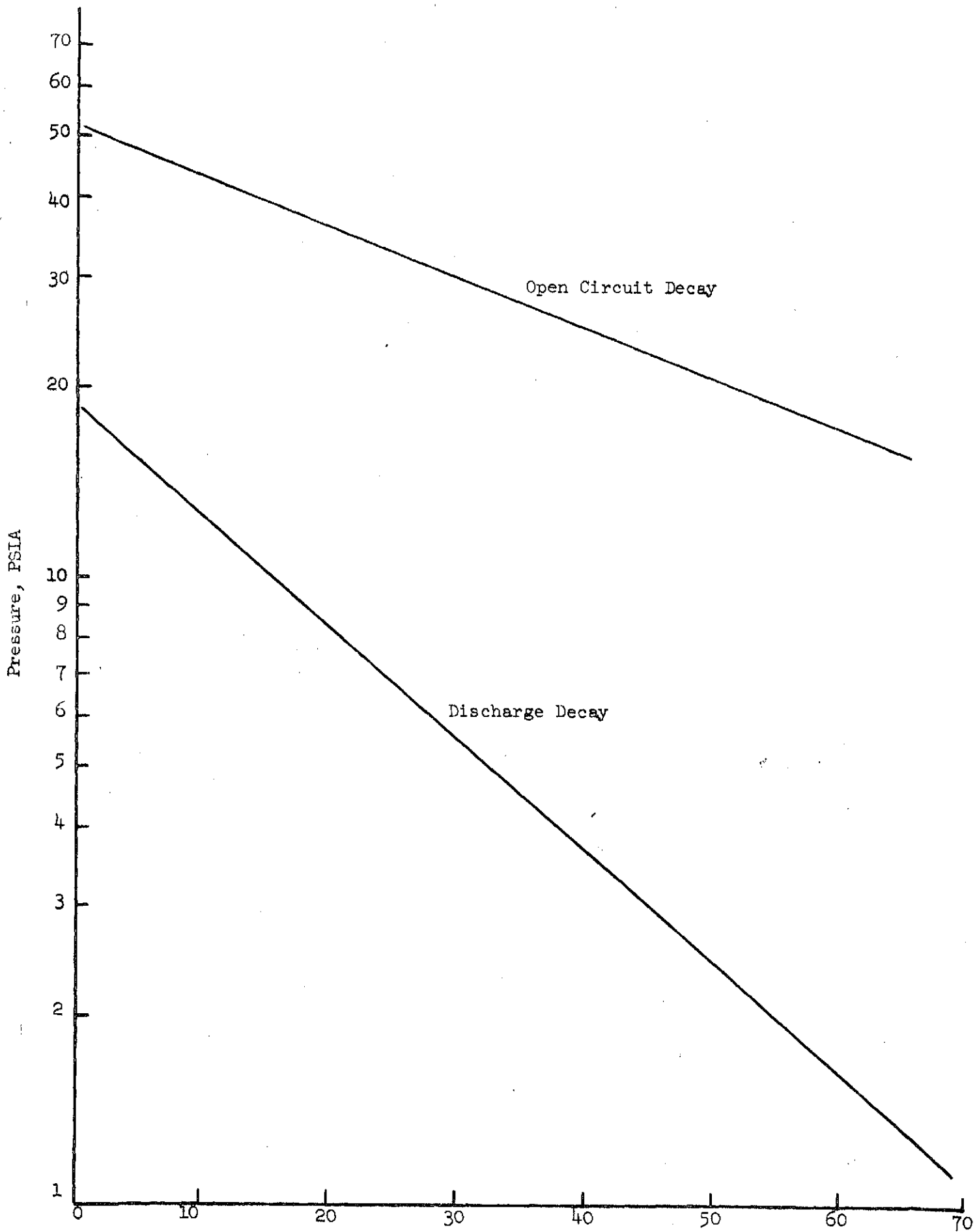
Figure -17- Effect of Charge Rate on Capacity

Pressure, Absolute PSI



Charge Current, Amperes

Figure -18- End of Charge Pressure, HNC100.3 S/N 1



Time, Minutes

Figure -19- Pressure Decay, HNC 100.3 S/N 1



Hence, it is concluded that the recombination reaction is slower on open circuit than it is when current passes through the cell. On open circuit the time required for the pressure to decay to one-half its initial value,  $t_{1/2}$ , is 38 minutes. During discharge it is 17 minutes. These numbers are of value only for comparison in the same cell. Such numbers cannot be used for comparison of different sizes of cells since the value largely depends on the gas volume within a cell, which in turn is design dependent.

## NEW TECHNOLOGY

While this program was carried out, eight new technology items were identified and reported to NASA. These items are briefly identified as follows:

### 1. Slurry Deaeration

The very slow rolling of slurry allows the slurry to release admixed air. Rolling rates are 0.2 to 1.0 turns per minute. The rolling drum capacity is 15 gallons, but is never more than 2/3 filled.

### 2. Oxamide Pore Former

An insoluble crystal decomposing into gaseous products at some temperature above ambient but below sintering was needed to control pores. The organic compound oxamide fulfills the characteristics needed.

### 3. Slurry Applicator

The machine designed for applying slurry to the grid has several key features. These are: (1) a pumping of slurry through to pores to ensure complete filling, (2) a set of guides to ensure that the grid is centrally located in the sinter and (3) a closed box-like structure to prevent admixture of air in the slurry scraped off the wet green plaque.

### 4. Temperature Ramp Profile

The need for a gradual increase of temperature as the plaque enters the furnace was recognized. This permits ablation of the binder and the pore former. It also provides the temperature for nickel oxidation.

## 5. Mechanical Strength Testing Apparatus

In response to a need for strength measurements independent of grid location a testing device was designed. The design measures the degree of degradation of sintered plaque to a coining force. A dead weight is applied to the plaque through a set of anvils and the degree of coining is measured.

## 6. Surface Area Measurements

The electrode/electrolyte interfacial area was measured using a pulsed potential step technique. To avoid errors due to faradaic processes a small potential step is applied to the test sample. The current required to bring the sample to a steady state at the new potential is measured and used for surface area calculations.

## 7. Oxygenation Prior to Sintering

It was found that admission of oxygen in limited quantity to the sintering furnace in that region where the temperature is still below sintering conditions improved the sinter. The first advantage was a better adhesion of sinter to the substrate. The second advantage was a uniform sinter that was strong. A third advantage is that the amount of oxygen can be precisely controlled.

Oxygenation is however common to other metallurgical sintering processes.

## 8. Design of the 100 AH Cell

The opposed terminals with large cross-sectional areas coupled with the thin plates conducts heat to the broad surface of the cell readily.

To further enhance this conduction the case of the cell is common with the negative electrodes. Enhancement of thermal conductivity was further achieved by elimination of air that could be entrapped in the electrodes.

## C O N C L U D I N G   R E M A R K S

The primary objectives of this program to develop the procedures and controls, and select the materials and equipment necessary to determine the production methods needed to secure uniform, consistent and defect-free plaque material has been completely attained. In fact, the results of the program exceed the goals in that not only is the plaque very uniform, defect free, and controllable, it is also quite strong and easily loaded with active materials.

In retrospect, some information of interest that developed during the course of this contract is:

- (1) Accurate control of the oxidizing atmosphere and temperatures in firing produces uniform sintering throughout the plaque and promotes adhesion of sinter to grid.
- (2) The addition of a pore former to the slurry apparently not only provides controlled vestibales within the plaque to allow easy access to the depth of the plaque but also contributes to the final strength.
- (3) Large voids in the plaque can be avoided simply by removing entrapped air by a simple rolling process.
- (4) Use of guide fingers in the doctor blade assembly to position the grid within the plaque.
- (5) Establishing that utilization of active material depends upon sinter porosity.
- (6) Establishing that the capacity is dependent upon charge rate, and that there is a significant fall-off of capacity at charge current densities below  $7 \text{ MA/in}^2$ .
- (7) Finding that air may be entrapped within the cell which should be eliminated. This thereby increases the volume of electrolyte injected into a cell, but there is no sacrifice in overcharge performance.
- (8) The oxygen recombination rate is slower on open circuit than it is during charge and discharge.

- (9) The surface area of plaque that is involved in the electrode/ electrolyte interface can be determined by a voltage pulse technique.
- (10) Recognizing that the  $\text{Cd}(\text{OH})_2$  precipitated during conversion from the nitrates acts as a dialysis membrane, has given rise to process change that makes the loading of the negative electrodes more uniform.
- (11) Tracing the stresses in the positive electrodes to the nature of the nickel hydroxide precipitated led to process changes that decreased blistering and thickening.



## RECOMMENDATIONS

The design of large size nickel cadmium cells can be altered to increase the specific energy to values in excess of 20 WH/lb without sacrifice of quality. Thus, the weight of a 100 AH cell targetted to deliver 125AH can be reduced to the neighborhood of six pounds. The specific recommendations to accomplish this follow, but it must be recognized that the strong uniform plaque developed under this program permit these recommendations.

1. Investigate the use of more porous and thicker positive plaque materials. The increased strength of the plaque developed under this program allows such a change. With more porous plaque the ratio of active material to inactive material is increased. Such changes must be made within the constraint that the utilization of positive active material decreases with increased porosity.
2. Investigate the use of more porous and thicker negative electrode compatible with the positive plaque material. As plaque becomes both thicker and more porous it tends to weaken. The optimal design characteristics should be sought.
3. Develop a computer program for design of battery cells. Changes in utilization and aspect ratios incur changes in separator volume and can weights. Optimization of batteries is too complicated to be done analytically, and an appropriate computer program can determine the optima.
4. Increase loading levels of the positive electrode by use of electrochemical deposition of active materials. Such methods allow loadings of  $1.8 \text{ g/cm}^3$  of void or higher while decreasing the incidence of defects due to blistering and decreasing the total amount of thickening.
5. Decrease sinter corrosion during impregnation. This may be done readily by maintaining the sinter at a cathodic potential whenever it is in contact with a corrosive environment.

## A C K N O W L E D G E M E N T S

The authors wish to acknowledge the contribution of many people who have helped in various ways to carry out the program. These include notably Mr. J. Fredrick Jansen, Mr. R. Oliver, Mr. M. van Leeuwen and Mr. Eugene Ralph. Measurements and fabrication were carried out by Dr. N. P. Yao; Dr. Vincent Puglisi, Mr. M. Milden, Mr. Walter Perrin, Mrs. Carlene Bonnell. Mr. Paul Ritterman's assistance in the final stages of the program was invaluable.

APPENDIX I

## APPENDIX I

### DERIVATION OF THE MAXIMUM CAPACITY RELATIONSHIPS

Formation cycling and other testing of positive electrodes under flooded conditions indicate that the dischargeable capacity exceeds the theoretical capacity. The theoretical capacity is obtained by obtaining the weight gain as  $\text{Ni}(\text{OH})_2$  after loading and basing the calculation on a one electron change. The reason for greater than theoretical values may be due either to conversion of some sintered metal or oxidation to a valence state greater than 3. Workers at Bell Telephone Laboratories reported that there is no apparent attack on the sinter.

It is not the purpose of this writing to ascertain the fundamental mechanism for values in excess of theoretical, but rather to note some isolated findings that appear to indicate a relationship between the dischargeable capacity and plaque characteristics.

Dr. Beauchamp and Maurer of BTL observe capacities exceeding theoretical loadings by 20%. Results in this laboratory on similar plaque were also 20% above theoretical. The plaque used was made by a slurry process and had a sinter porosity of 72%.\* Plates made using plaque made by the loose powder method yielded 5% more capacity than the theoretical value. These plaques were 82% porous. Many years ago similar plates were found to yield values of 2 to 3% above theoretical values. Recently, a third point has been added. Heliotek produced plaque with a sinter porosity of 75% and obtained a formation capacity 15% above the theoretical. Admittedly, these findings did not come from a controlled experiment and require substantiation, but they are based on experiments by several groups. These data are plotted in Figure A-1. A straight line was eyeballed through these data points. The equation for the line is:

---

\*Porosities are given based on the sinter neglecting the presence of the grid. This procedure eliminates consideration of thickness and the grid.

CAPACITY OF DEPENDENCE ON SINTER POROSITY

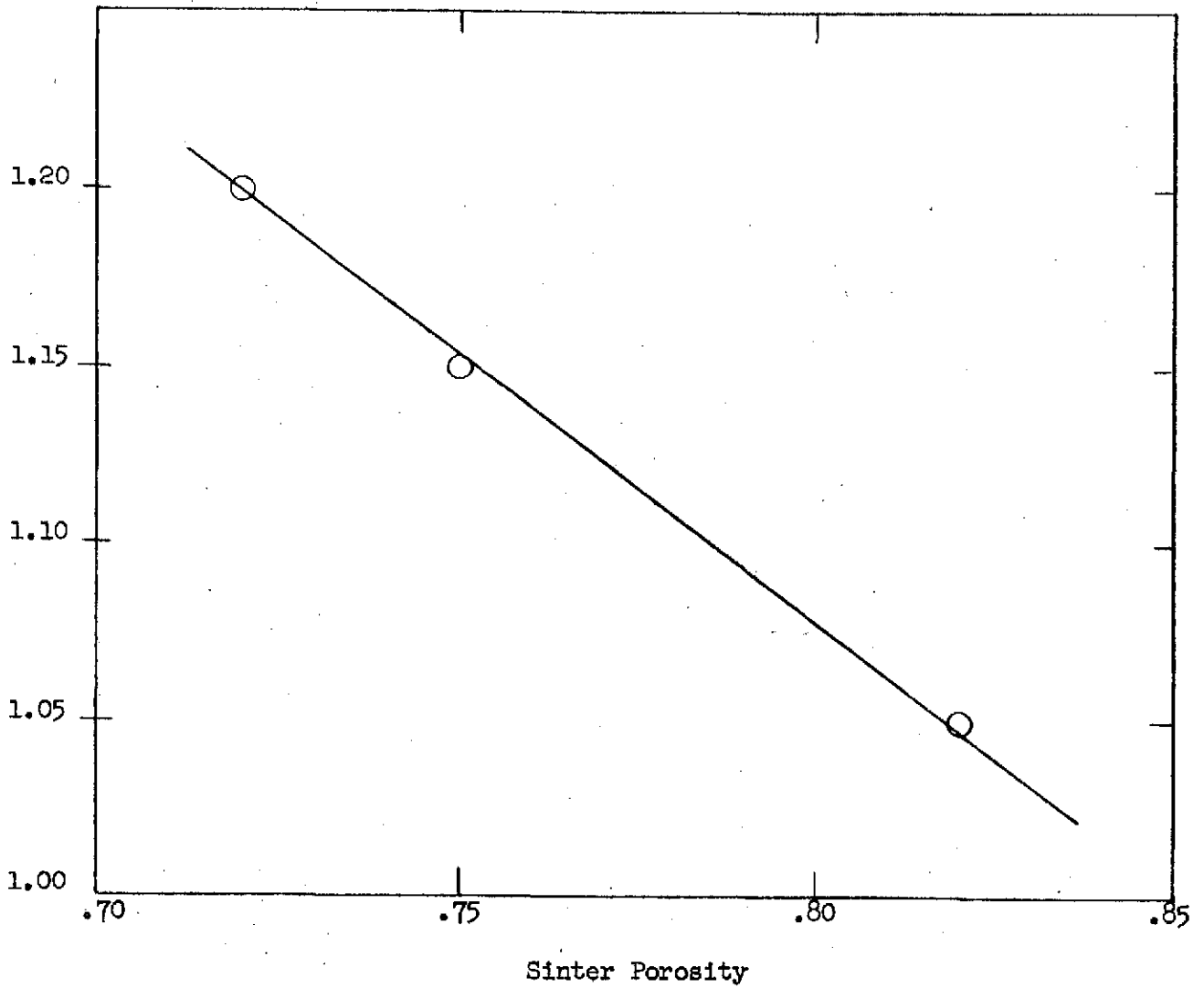


FIGURE A1-a

$$(1) \quad \epsilon = 2.2 - 1.4p,$$

where  $\epsilon$  is the utilization and  $p$  is the sinter porosity.\*

Consider now a plaque of unit area and a required thickness  $t$ . The volume of the plaque is, therefore,  $t$ . The void volume is the difference between the total volume and that volume occupied by metallic nickel which is  $w/\phi$  where  $w$  is the weight of the plaque and  $\phi$  is the density of nickel. The plaque porosity is given by

$$(2) \quad P_p = \frac{t - \frac{w}{\phi}}{t}$$

but equation 2 is plaque porosity and not the sinter porosity. To change this sinter porosity, some subtractions are necessary. Let  $w_g$  be the grid weight, then

$$(3) \quad p = \frac{t - \frac{w}{\phi}}{t - \frac{w_g}{\phi}}$$

and equation 3 yields the sinter porosity. It should be noted that the term  $t - w/\phi$  is the void volume.

Let  $K$  be the loading level. The loading of the plaque is simply the product of  $K$  and the void volume which is  $K(t - \frac{w}{\phi})$ . The dischargeable capacity is given by the product of the utilization,  $\epsilon$ , and the loading level which is:

$$(4) \quad C = K \left( t - \frac{w}{\phi} \right) \epsilon,$$

where  $c$  is the dischargeable capacity observed in flooded conditions. Let  $t - \frac{w_g}{\phi} = T$ , which is assuming not only a required and constant plaque thickness, but also a constant grid structure and weight. These are

---

\*Figure 1b includes data on page 51 and page 199 from the recent report AFAPL-TR-72-35, H.H. Kroger, "Nickel Hydroxide Battery Electrode Development," dated July 1972.

reasonable assumptions. Substituting  $pT$  for  $(t - w/\phi)$  and using equation 1, equation 5 is obtained. Equation 5 is the equation

$$(5) \quad C = K p T (2.2 - 1.4p).$$

of a parabola and may be differentiated twice.

$$(6a) \quad \frac{dc}{dp} = 2.2KT - 2.8KTp$$

$$(6b) \quad \frac{d^2c}{dp^2} = -2.8KT$$

Setting equation 6a to zero yields an extremum which equation 6b shows to be a maximum. Capacity is maximized when the sinter porosity is 78.5%.